TECHNICAL REPORT No. 50

ON THE DEVELOPMENT OF OROGRAPHIC CYCLONES

by

Djuro Radinovic*

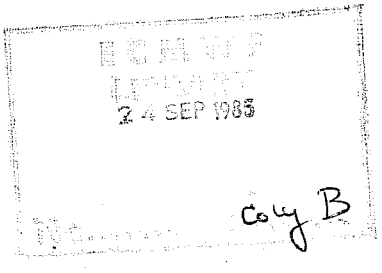

June 1985

* Visiting Scientist on leave from
Faculty of Sciences,
University of Belgrade,
Belgrade, Yugoslavia

C O N T E N T S

1. INTRODUCTION

When studying various synoptic aspects of cyclone development, Petterssen and Smebye (1971) identified two types of extratropical cyclones:

- Type A is the well known amplifying frontal wave, which is known to produce kinetic energy through a reduction of baroclinicity within its own domain.

- Type B is initiated by a finite disturbance in the upper troposphere; its intensification is accompanied by an augmentation of the baroclinicity and the import of kinetic energy, mainly from the jet stream region.

Detailed descriptions of these two types of extratropical cyclone development will not be given here.

Evidence derived from many studies (e.g. Radinović, 1965; Speranza, 1975; Buzzi and Tibaldi, 1978; Illari, Malguzzi and Speranza, 1981; McGinley, 1982) and synoptic experience have gradually accumulated in support of the view that the mechanism of lee cyclogenesis is somewhat specific and should be considered as a different type of cyclogenesis. For convenience the notation introduced by Peterssen and Snebye will be used, and we shall refer to this mechanism as Type C. This categorisation, it is believed, will help clarify the mechanism of cyclogenesis since a single theory of extratropical cyclone development still does not exist.

During the last two decades, numerous case studies of orographic cyclones have revealed some of their specific features: the orographic blocking of the cold air mass; the deformation of the upper trough as it approaches the mountains; the particular evolution of the baroclinicity and vorticity, as well as the energy transformations; the various stages of development. The most comprehensive case study has been carried out by McGinley (1982), from which a clear conceptual model of orographic cyclogenesis has emerged.

If we assume that the specific features of orographic cyclones, described in most case studies, are present and pronounced in the majority of individual cases of cyclogenesis, then they should be evident in the mean fields derived from the ensemble of cyclones encountered in the ALPEX period. The main purpose of this study is to use this methodology to show that the mechanism of lee cyclogenesis is somewhat different from that responsible for Types A and B.

2. STATISTICS

During the ALPEX Special Observing Period (March-April 1982) eight cases of cyclogenesis in the lee of the Alps occurred. All these cases have been briefly reviewed by Buzzi and Tosi (1982), while some cases have been studied in more detail (Jansa and Ramis, 1982; Dell'Osso and Tibaldi, 1982; Pham, 1982; Mattocks, 1982; Lüdecke, 1982).

Using the International ALPEX Data Bank, a series of hand analysed charts for all eight cases of cyclogenesis has been produced. These have been used to study the statistical behaviour of the orographic cyclones in the western Mediterranean.

Using the criterion that the initiation of cyclogenesis takes place three hours before a closed isobar is observed, and the time of disappearance is three hours after the last closed isobar vanishes, it was found that the cyclones which occurred during the ALPEX Special Observing Period (SOP) were relatively long lasting. Table 1 shows that the shortest duration was two days and the longest five days, while the average duration of all eight cyclones was 3.8 days.

Table 1. Duration of cyclones which occurred during the ALPEX SOP

Case No.	1	2	3	4	5	6	7	8
Duration (days)	4.6	3.6	2.8	5.0	5.0	4.4	3.2	2.0

By following the positions of the centres of the cyclones, it is found that the majority of cyclones cross the Mediterranean and disappear over the Middle East. Only in one case does a cyclone develop and decay entirely in the western Mediterranean.

There is a great variation in the speed of movement of the various cyclones, but during the first 24 hours of development there appears to be a characteristic behaviour, as shown in Table 2. During the 6 hours after cyclogenesis the cyclones are almost stationary. Thereafter they begin to move and reach a maximum speed of about 35 km/hour during the period 12-18 hours; later the speed decreases.

Table 2. Movement of cyclone centre during the first 24 hours of cyclogenesis

Period of cyclogenesis (hours)	0-6	6-12	12-18	18-24
Average distance moved (km)	25	175	205	140

The movement of the cyclones is closely related to the mechanism of lee cyclogenesis. During the first 6 hours the development is closely connected with the mountain range, but in the next 6 hours the cyclone develops aloft, above the mountains, and the steering effect becomes strong enough to move the cyclone with the upper flow. After 12 hours of cyclogenesis the cyclones usually develop vertically, up to the middle of the troposphere, and reach

their maximum speed. Later the cyclones continue to develop vertically into the upper troposphere and expand horizontally in the lower layers. This causes a decrease of the steering effect and the cyclones slow down.

This explanation is supported by the data contained in Table 3 which shows the time lag in the vertical development. Note that the first closed contour at 850 mb occurs on average 6 hours after the first one appears at the surface; the lag at 300 mb is 27 hours.

Table 3. Time lag (to the nearest 3 hours) in the lee cyclone vertical development.

Level (mb)	850	700	500	300	1000-500
Time lag (hr)	6	9	18	27	24

This study has also shown that the tilt and the form of the vertical axis of the lee cyclones vary with time. In the growing stage the vertical axis from the surface up to the mountain top is nearly normal to the earth' surface because of the fall of the heights of the standard pressure levels which are mainly caused by a surface pressure fall due to the absence of the cold air advection in that layer. The position of the centre of the closed contours at 500 mb and above depends primarily on the cold air advection and the horizontal advection of vorticity. Therefore the vertical axis is usually orientated towards the centre of cold advection and is more tilted in the upper layers than the lower ones. However, when the cyclone is moving, the vertical axis in the lower layer becomes more tilted. In the mature stage there is hardly any tilt in the vertical axis.

As a measure of cyclone intensity, the geostrophic circulation around the cyclones centres has been calculated (Radinović and Lalic, 1959). The circulation was evaluated using the finite difference form of the Laplacian of geopotential height on a 500 km grid. Table 4 shows the intensity of all eight cyclones at 5 isobaric levels when the cyclones reach their maximum development.

Table 4. Maximum cyclone intensity, as measured by $\nabla^2 Z$, reached during the cyclone activity in the ALPEX SOP.

Case No. \ Level	1000	850	700	500	300
1	52	30	42	28	40
2	60	40	44	36	40
3	32	30	28	16	-
4	36	30	27	28	-
5	23	28	26	42	24
6	32	28	35	31	48
7	45	33	38	67	82
8	38	40	40	42	-

Here, d=500 km is taken as 1.

Following the criteria described by Radinović(1965a), cyclones with a Laplacian of 16 gpd/(500 km)^2 are described as small low pressure systems, those with values in the range 17-32 gpd/(500 km)^2 are moderate while cyclones

with larger values are described as having great intensity. Table 4 shows that according to these criteria there are three moderate cyclones and five with great intensity. Furthermore, in the first four cases the greatest intensity occurs at the surface, while in the other cases the intensity is largest aloft.

A detailed analysis of these situations also reveals that in seven cases there is a lag with height of the appearance of maximum intensity - the lag at 850 and 700 mb is about 6 hours, and about 12 hours at 500 mb. In case 7 the reverse happened, the maximum intensity first appears aloft and then at the surface. This case was completely different from the others because there was a cold pool on the northwest slope of the Alps which formed before cyclogenesis occurred.

In order to have a better understanding of the dynamics of lee cyclogenesis, the pressure and geopotential changes in different sectors of the cyclones have been examined. The changes were measured at the centre of the cyclone (denoted by 0) and at four other points which were 500 km towards the west (W), south (S), east (E) and north (N) of the cyclone centre. Two 12 hour periods from the beginning of cyclogenesis were used, with the period being taken between the nearest synoptic hours. The results for all eight cases are presented in Tables 5 and 6.

Table 5. Average geopotential changes during the first 12 hours of cyclogenesis (gpm)

Level \ Points	0	W	S	E	N
1000	-64	34	-20	-32	36
850	-52	2	-24	-28	-10
700	-53	-16	-19	-28	-29
500	-76	-44	-19	-38	-69

Table 6. Average geopotential changes during the period 12-24 hours after cyclogenesis starts (gpm)

Level \ Points	0	W	S	E	N
1000	-40	30	-19	-28	45
850	-52	2	-30	-21	30
700	-68	-14	-44	-29	14
500	-95	-39	-65	-39	-8

Table 5 shows that the greatest fall of geopotential occurs at the centre of the cyclone at all levels. Also the magnitude of the surface geopotential fall at the centre is about twice the rise in the northern and western sectors, showing that the pressure fall due to cyclogenesis is more pronounced than the effect of the cold air accumulation on the windward side of the mountain barrier. Further, the greater fall of geopotential at 500 mb compared to that at 1000 mb illustrates that during the first 12 hours of cyclogenesis cold advection takes place aloft over the centre of the cyclone.

From Table 6 it may be seen that in the period 12-24 hours after the cyclone first forms, the pressure at the centre of the cyclone is still falling. However, the fall increases with height in the troposphere, showing that in this period both cold air advection and cyclonic vorticity advection play an important role in the vertical development of the cyclone. In the western and eastern sectors of the cyclone the geopotential changes are similar in both periods. This is not so in the southern sector where there is a marked enhancement with time of the geopotential fall aloft and this shows that cold air and cyclonic vorticity in the middle of the troposphere have already moved into this region. A very marked increase in surface potential in the northern sector of the cyclone, which extends up to nearly 500 mb, indicates that the cold air advection on the windward side of the Alps decreases or stops, while pressure aloft continues to rise dynamically (i.e. due to mass convergence aloft).

An analysis of cross-sections through the cyclone in various directions has revealed some interesting features; some of these are summarised in Table 7.

Table 7 Average maximum wind speed in the zonal and meridional cross-sections at (a) the time of appearance of cyclogenesis and (b) 12 hours later. Zonal cross-section made along 47°N and meridional ones along 10°E

Cross-section	Time	Direction	Speed m/s	Position	Height km
Zonal	a	S	16	10.5°E	7.5
	b	S	15	13.0°E	6.8
Zonal	a	N	30	2.5°W	7.1
	b	N	40	1.0°E	7.2
Meridional	a	W	37	46.5°N	7.5
	b	W	32	42.2°N	7.5

The zonal cross-sections show that at the onset of cyclogenesis there is a southerly wind component over the Alps. The maximum speed occurs at about 7 km, but its magnitude varies greatly from case to case (2-30 ms). At the same time the winds at the same level about 1000 km to the west have a northerly component with approximately twice the speed. The maximum northerly component of wind is over the Alps usually 12-24 hours after cyclogenesis has started.

From the meridional cross-sections it may be seen that during the initial stages of cyclogenesis, winds with a westerly component are dominant over the Alpine region. The maximum speed is about 7 km above the northern slopes of the Alps with an average speed of about 37 m/s in all eight cases. This westerly jet shifts about 500 km southwards during the next 12 hours; during this process the altitude of the jet remains the same, but the speed decreases by about 5 m/s.

3. DYNAMICAL FEATURES

The horizontal wind components at the beginning of cyclogenesis and 12 hours later have been analysed for all cases. The mean values of the zonal and meridional components, as well as their 12 hour differences, are shown in Figs. 1-6 for the 1000 mb, 850 mb, 700 mb and 500 mb levels. Figs. 7-12 show the corresponding charts of divergence and vertical velocity. We will now discuss the pertinent features of the fields.

Zonal wind component

At the beginning of cyclogenesis, as seen in Fig. 1, the mean zonal wind component at the surface is generally weak (1-4 m/s). The largest speeds of 2-4 m/s are only found over France and northeast Spain, while the negative values over central and northern Italy show that slight convergence already exists at the surface. At 850 mb the belt of high zonal wind components, reaching 12-14 m/s, extends westward and northward of the Alps, while there is a minimum of less than 2 m/s in the northern Adriatic. This distribution, with a strong gradient over the mountain range, shows the real effect of the Alps. Higher up, the wind speed gradient becomes less sharp over the mountains. However the speed over and to the north of the Alps increases, while in the central and southern parts of the western Mediterranean basin there is little change.

Fig. 2 shows that 12 hours later the belt of high zonal wind component shifts southwards; the maximum speed at lower lvels is now located over Corsica, and at higher levels over the Gulf of Lyon.

The difference between the zonal wind components at the beginning of cyclogenesis and 12 hours later is given in Fig. 3. The centre of the maximum

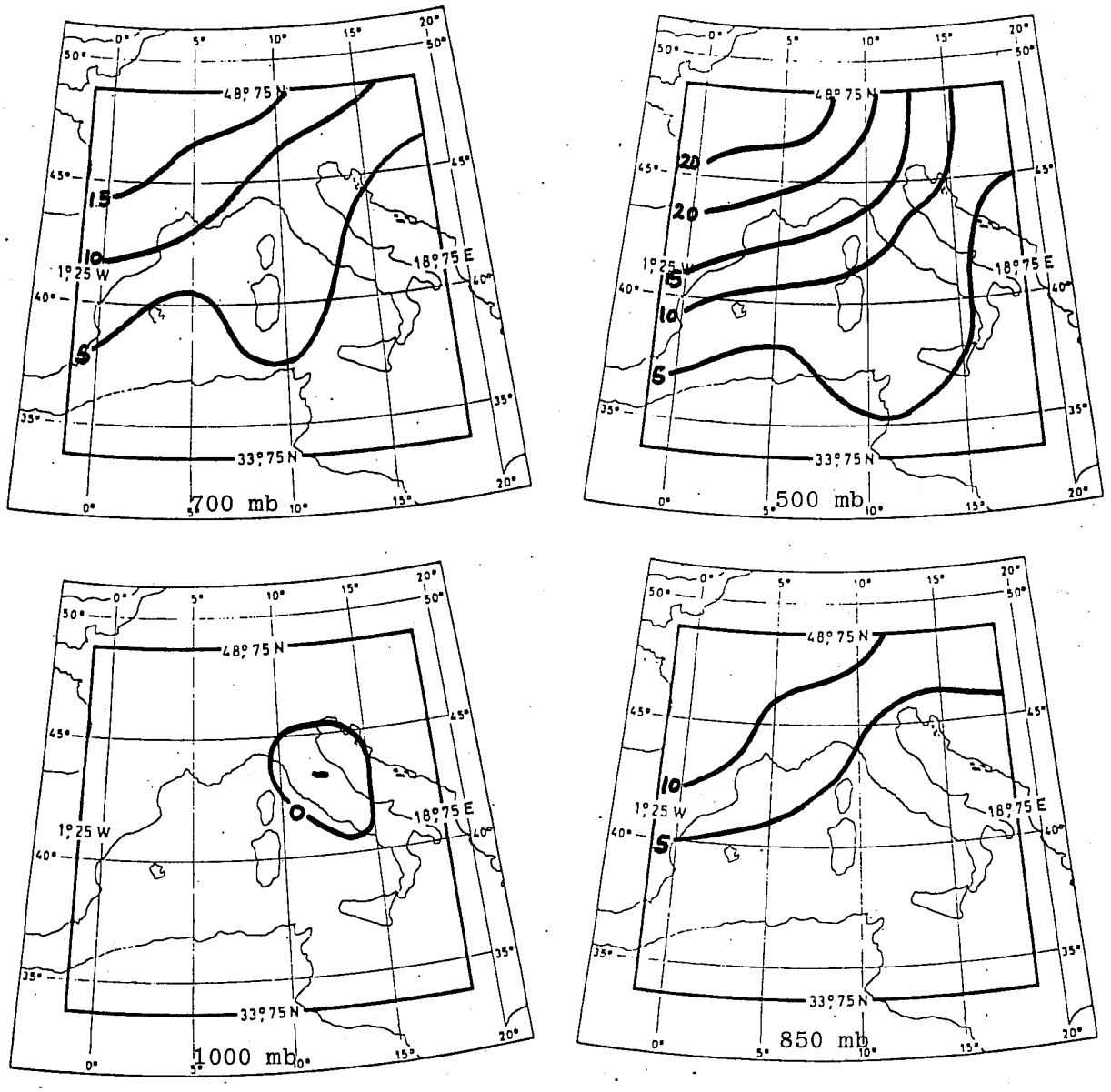

Fig. 1 Mean zonal wind component (m/s) at the beginning of cyclogenesis in the lee of the Alps observed during the ALPEX SOP.

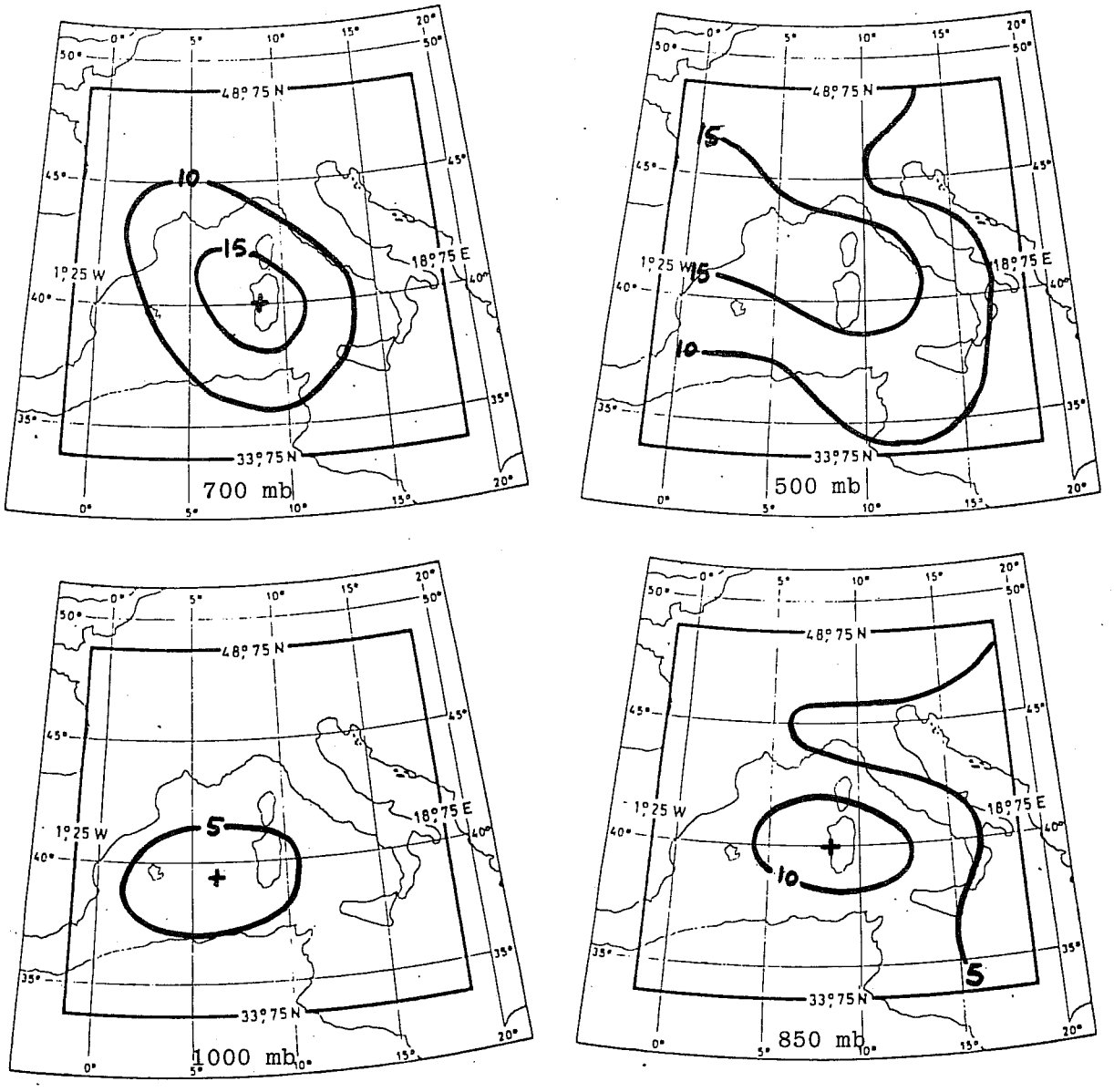

Fig. 2 Mean zonal wind component (m/s) 12 hours after the beginning of cyclogenesis in the lee of the Alps observed during the ALPEX SOP.

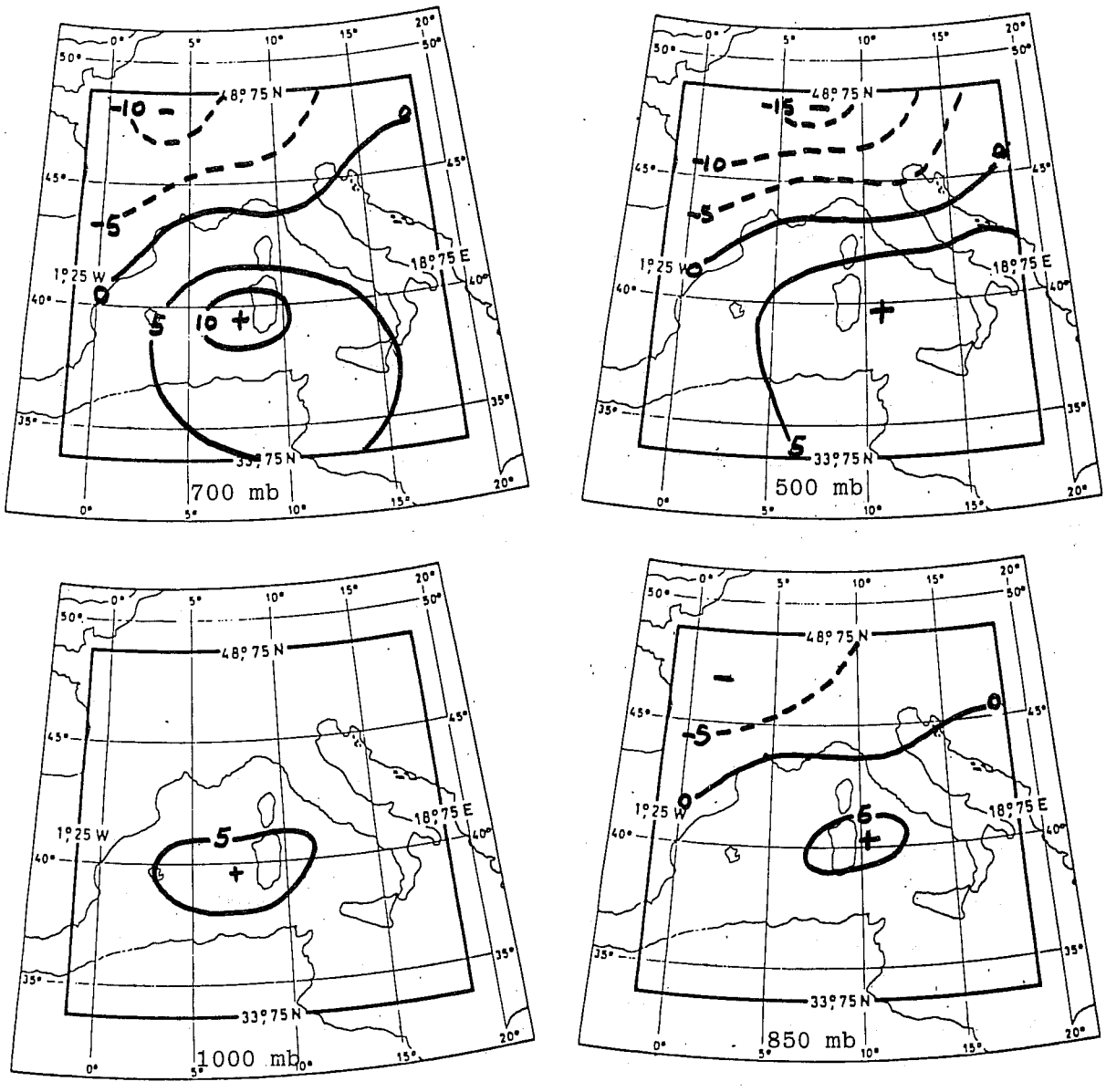

Fig. 3 Change of mean zonal wind component (m/s) during the 12 hours after the beginning of cyclogenesis in the lee of the Alps observed during the ALPEX SOP.

positive change of speed is located near Corsica, and appears to be the result of the intensification of the zonal wind in the southern sector of the low level cyclone in the lee of the Alps. The negative values in the northern part of the area are considered to be the result of two effects: at lower levels the zonal wind component decreases due to the blocking of cold air, while at higher levels the decrease is caused by the meridional shift of the belt of high winds.

Meridional wind components

The meridional wind components at the beginning of the cyclogenesis are shown in Fig. 4, and this clearly shows the diffluent flow pattern. At the surface the meridional flow is very weak everywhere, less than 1 m/s. Higher up at 850 mb and 700 mb there are two centres of high meridional component: a positive centre to the north of the Alps and a negative one over the Tyrrhanian Sea. These centres correspond to the northern and southern branches of the diffluent flow pattern. However, at the 500 mb level, due to strong zonal wind, the northern branch of the diffluent flow is absent, and the positive centre of the meridional component disappears.

12 hours after cyclogenesis started the distribution of meridional wind component has completely changed (Fig. 5). At low levels there now exists two centres of high speed: a positive centre over the central part of Italy and a negative one over the Rhone Valley. Both these reflect the well developed circulation of the low level cyclone. Higher up, these centres are located further north and are connected with the upper trough whose axes has just reached the Alpine massif. It is worthy of note that at all levels the northerly component is much stronger than the southerly one. The transformation of the prevailing diffluent flow pattern at the onset of

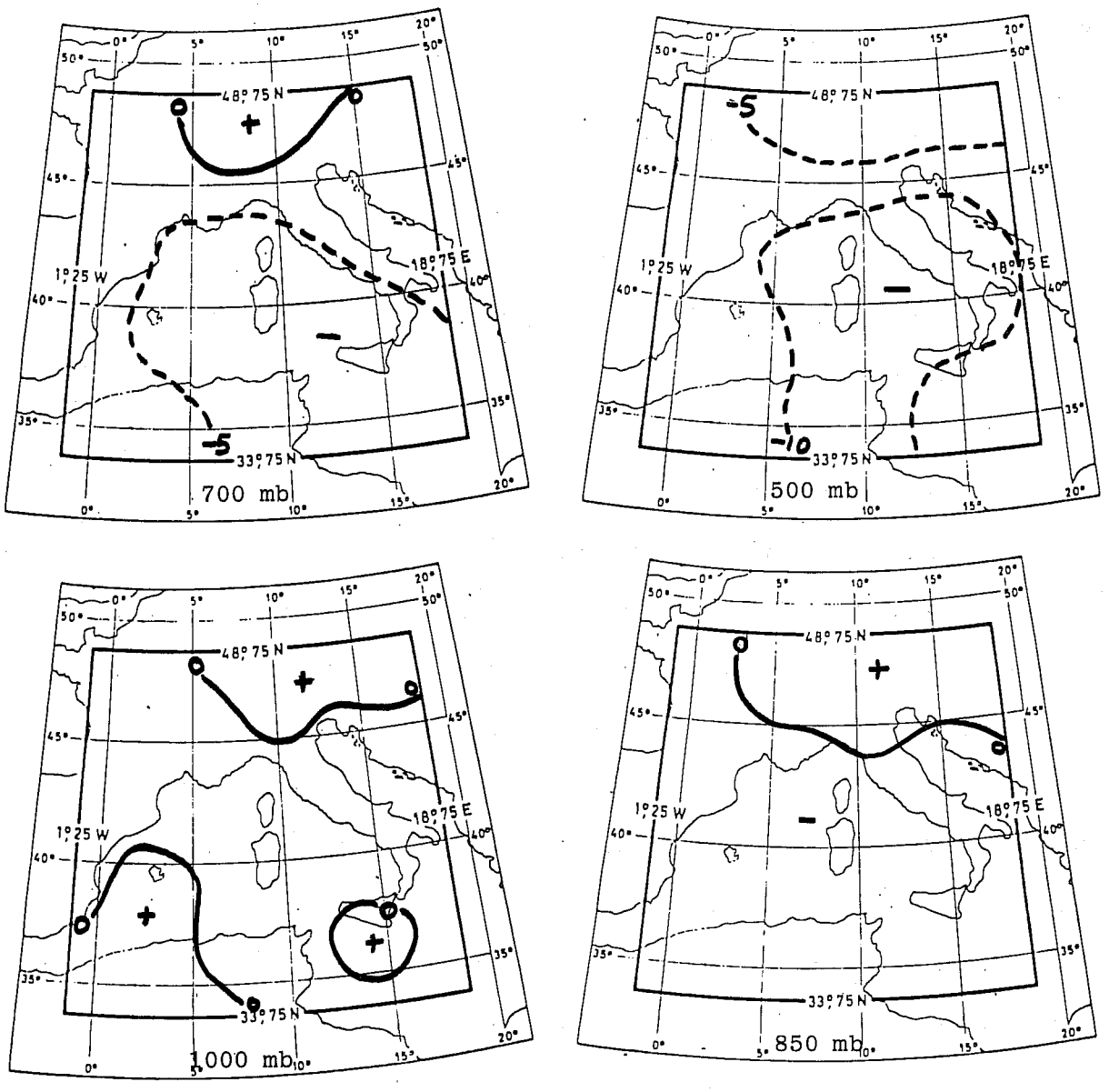

Fig. 4 Mean meridional wind component (m/s) at the beginning of cyclogenesis in the lee of the Alps observed during the ALPEX SOP.

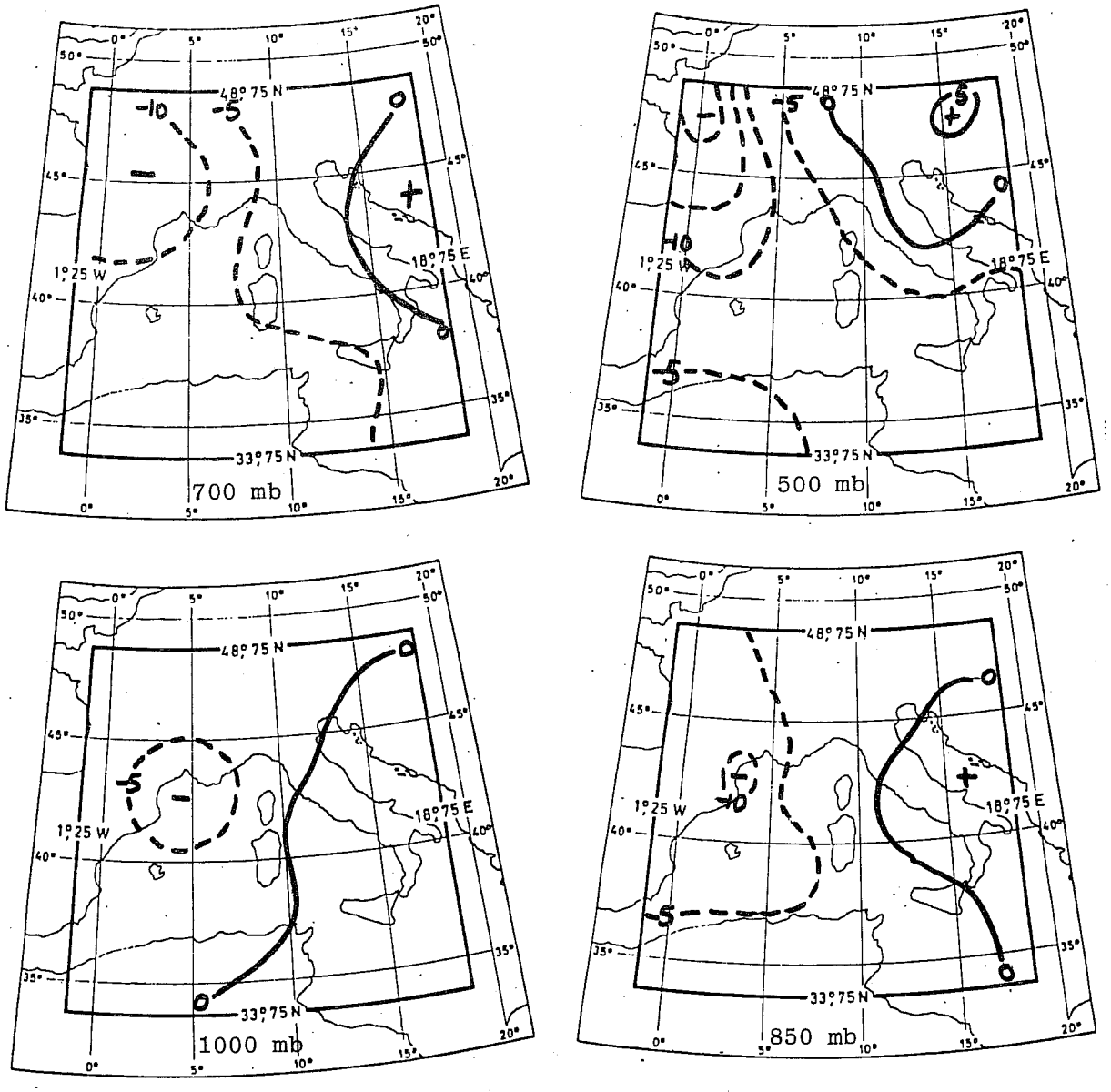

Fig. 5 Mean meridional wind component (m/s) 12 hours after the beginning of cyclogenesis in the lee of the Alps observed during the ALPEX SOP.

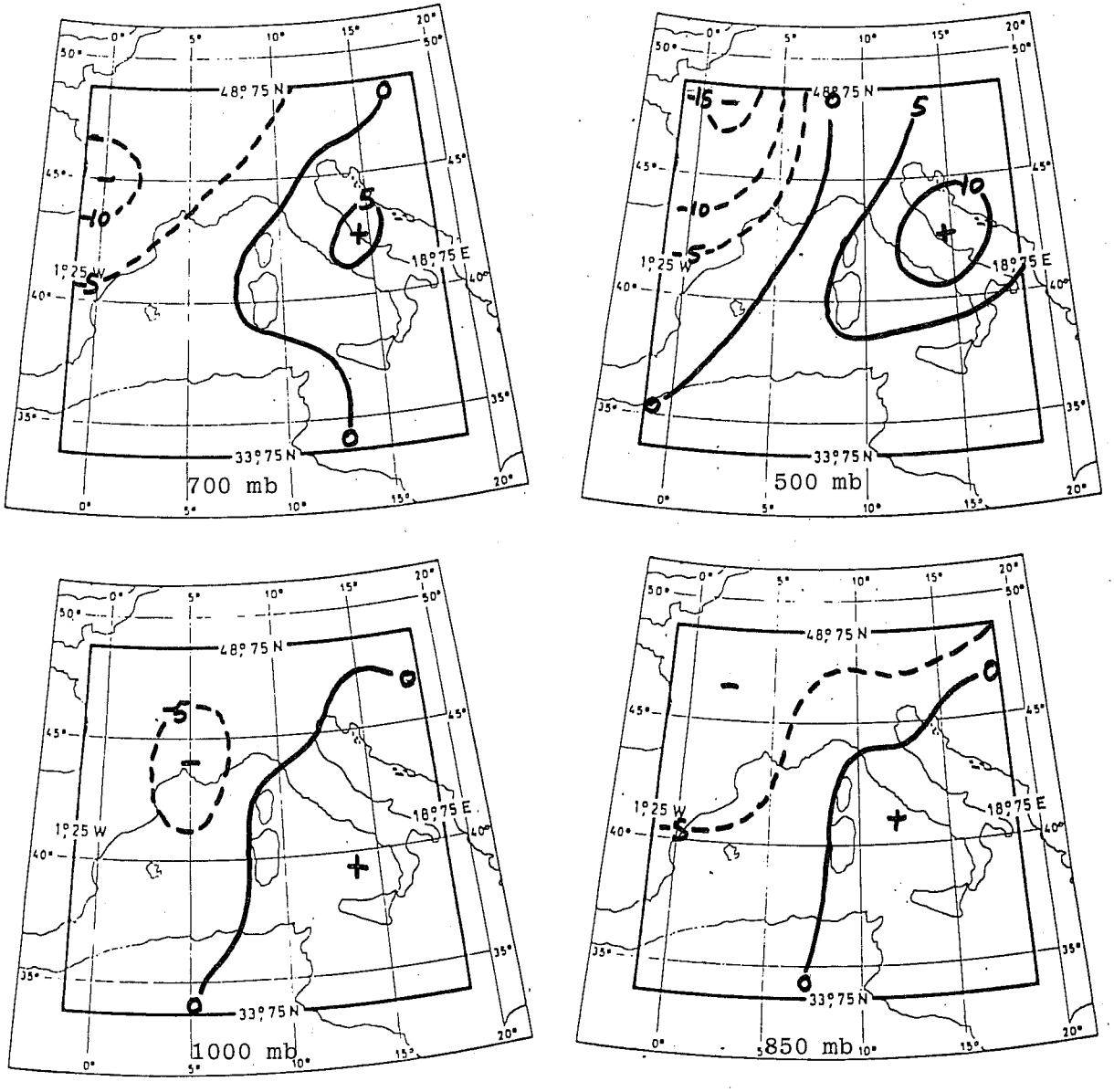

Fig. 6 Change of mean meridional wind component (m/s) during the 12 hours after the beginning of cyclogenesis in the lee of the Alps, observed during the ALPEX SOP.

cyclogenesis to a combination of a low level cyclonic circulation and upper trough 12 hours later is illustrated very clearly by the meridional wind component change shown in Fig. 6.

Divergence

Initially (Fig. 7) there are two distinct features in the divergent pattern at low levels (1000 mb and 850 mb): the high negative values over the western parts of the Alps and the high positive values over the eastern part. In mid-troposphere (700-500 mb) the belt of negative values of divergence spreads over most of the western Mediterranean basin, while the area with positive values covers the whole western and northwestern parts of the Alpine region. After a further 12 hours there is a marked change in the divergence pattern, as seen in Fig. 8. The centre of negative values in the lower levels is now located in the Gulf of Genoa, while the northern and northwestern parts of the Alps are covered by positive values. In the middle troposphere the negative centre shifts towards the Alps, and a belt of positive divergence develops in the western Mediterranean. The divergence in the upper levels of the troposphere at this stage of development is not very uniform.

The change of sign and intensity of the divergence at different levels during the first 12 hours of cyclogenesis is illustrated in Fig. 9. This gives a clear description of the divergence evolution in the initial stage of orographic cyclone development.

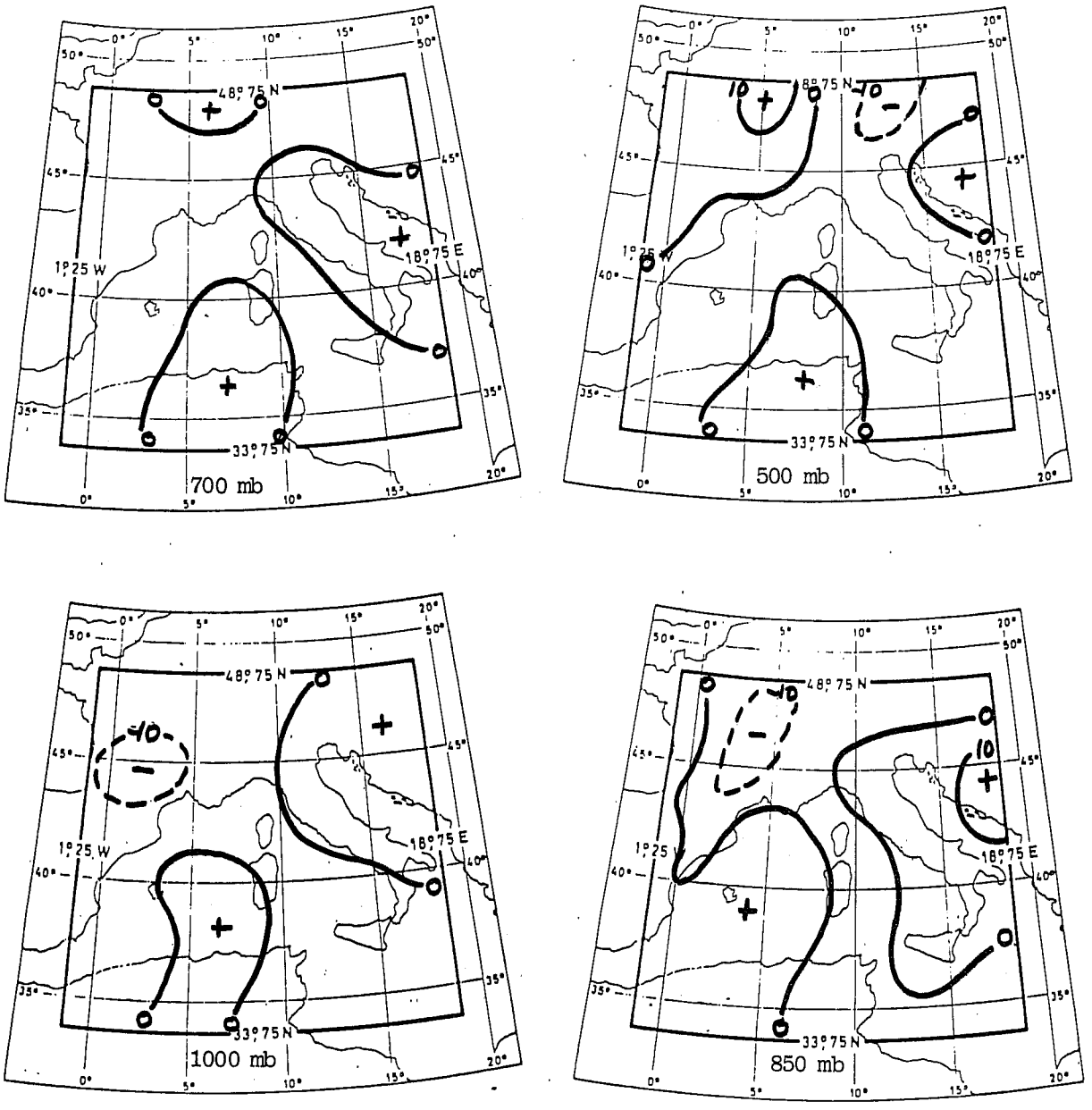

Fig. 7 Mean wind divergence ($10^{-6}s^{-1}$) at the beginning of cyclogenesis in the lee of the Alps observed during the ALPEX SOP.

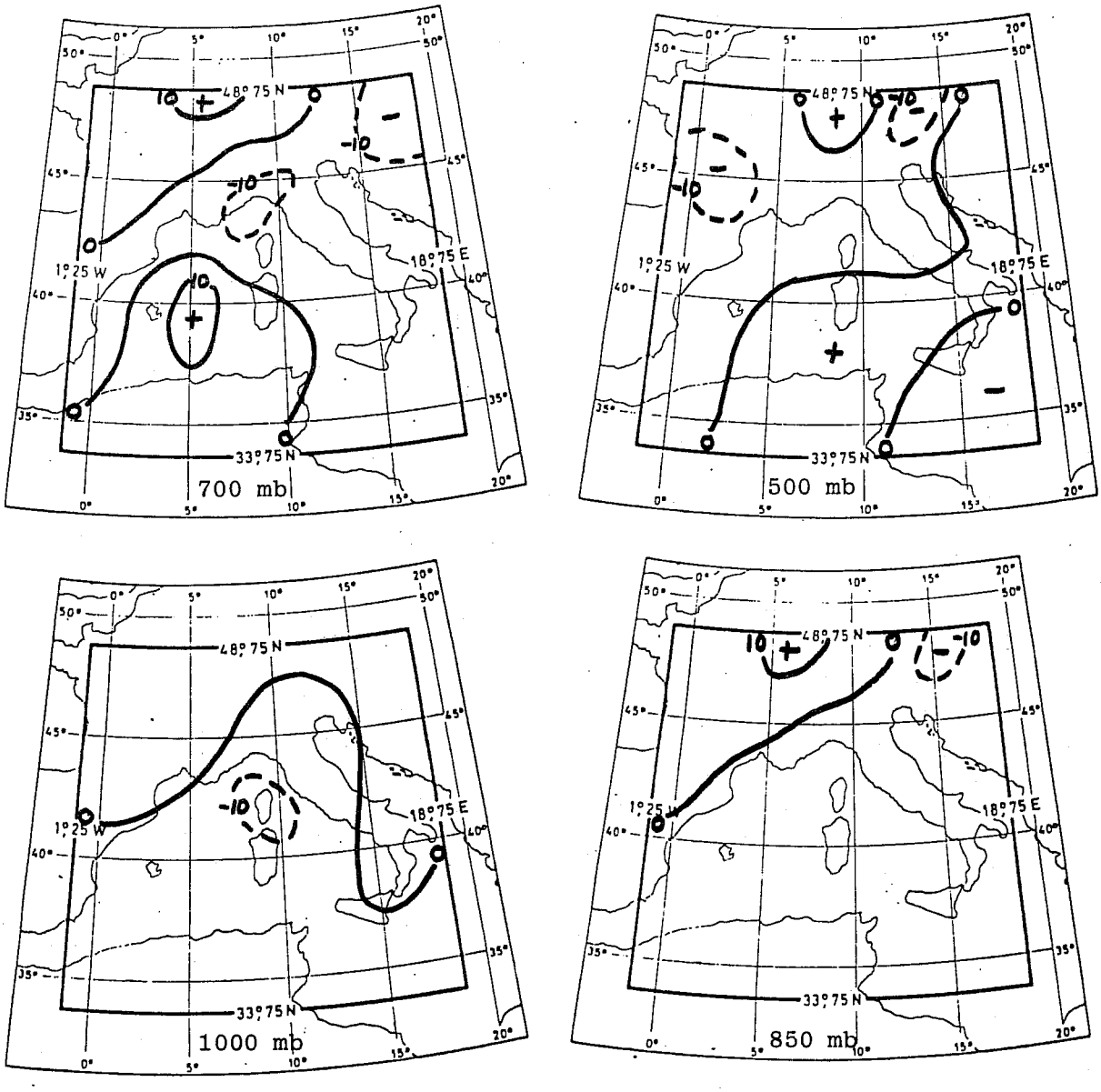

Fig. 8 Mean wind divergence ($10^{-6}s^{-1}$) 12 hours after the beginning of cyclogenesis in the lee of the Alps observed during the ALPEX SOP.

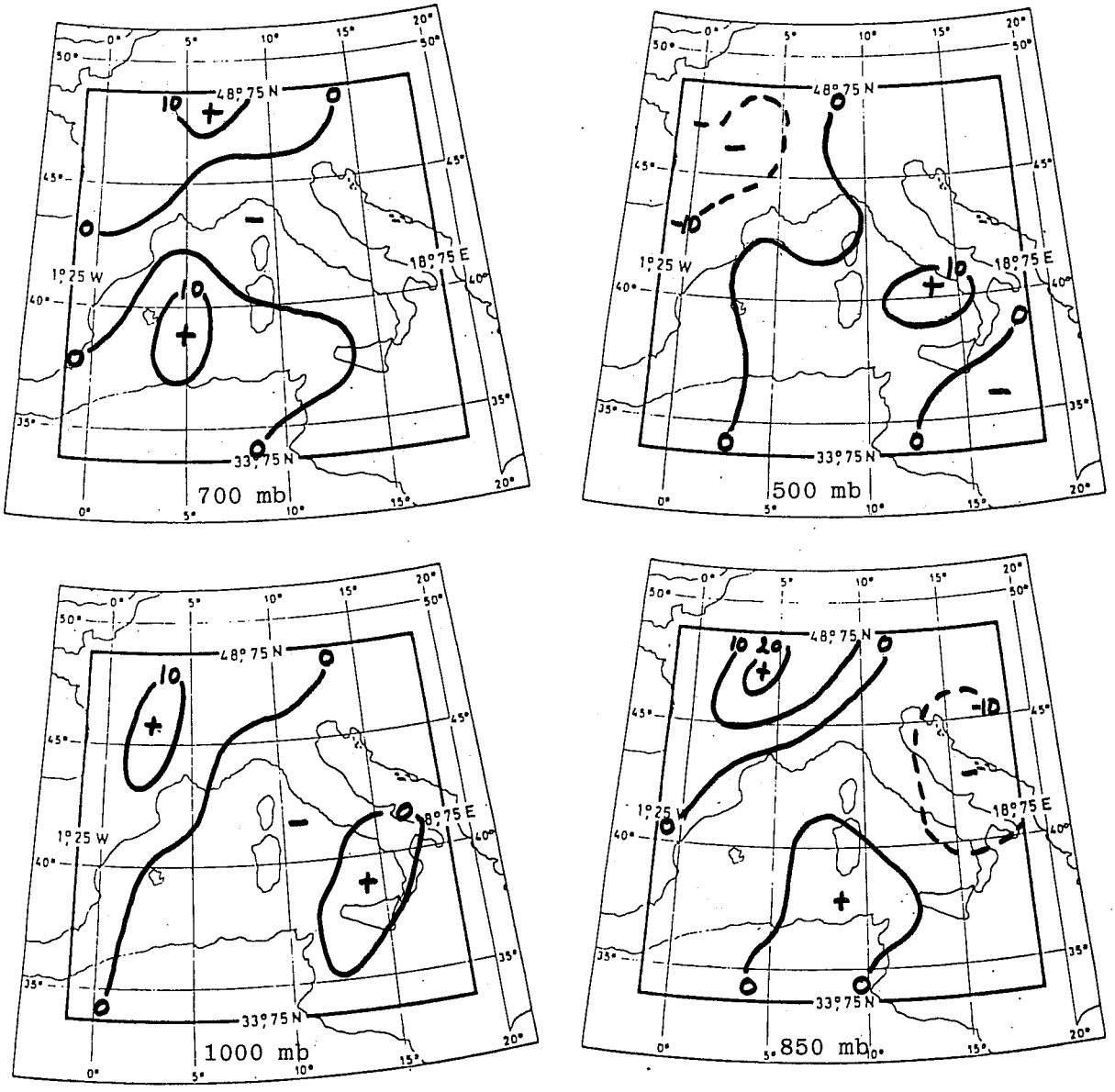

Fig. 9 Change of mean wind divergence ($10^{-6}s^{-1}$) during the beginning of cyclogenesis in the lee of the Alps observed during the ALPEX SOP.

Vertical velocity

The 'omega' vertical velocity at the onset of cyclogenesis is shown in Fig. 10. There are three main features:

- the area of descent (positive values) covering the Adriatic and the western part of Yugoslavia which strengthens from the surface to 500 mb.

- the area of ascent (negative values) over the western part of the Alps which increases up to 500 mb.

- the area of ascent over the northwestern part of the Alps which is weak at low levels and intensifies from 700 mb upwards.

The most prominent feature is the omega field 12 hours after cyclogenesis has started is the development of ascending motion over the Ligurian Sea (Fig. 11). This reflects the intensification and vertical development of the cyclone in the Gulf of Genoa. Also note that from 700 mb upwards the three areas of descent surrounding the ascending air intensify.

Fig. 12 gives the change in omega during the first 12 hours of cyclogenesis. This illustrates the strong tendency for there to be ascent over the Ligurian Sea, northern Italy and the Adriatic, as well as descent over the Alps and the southern parts of the west Mediterranean basin.

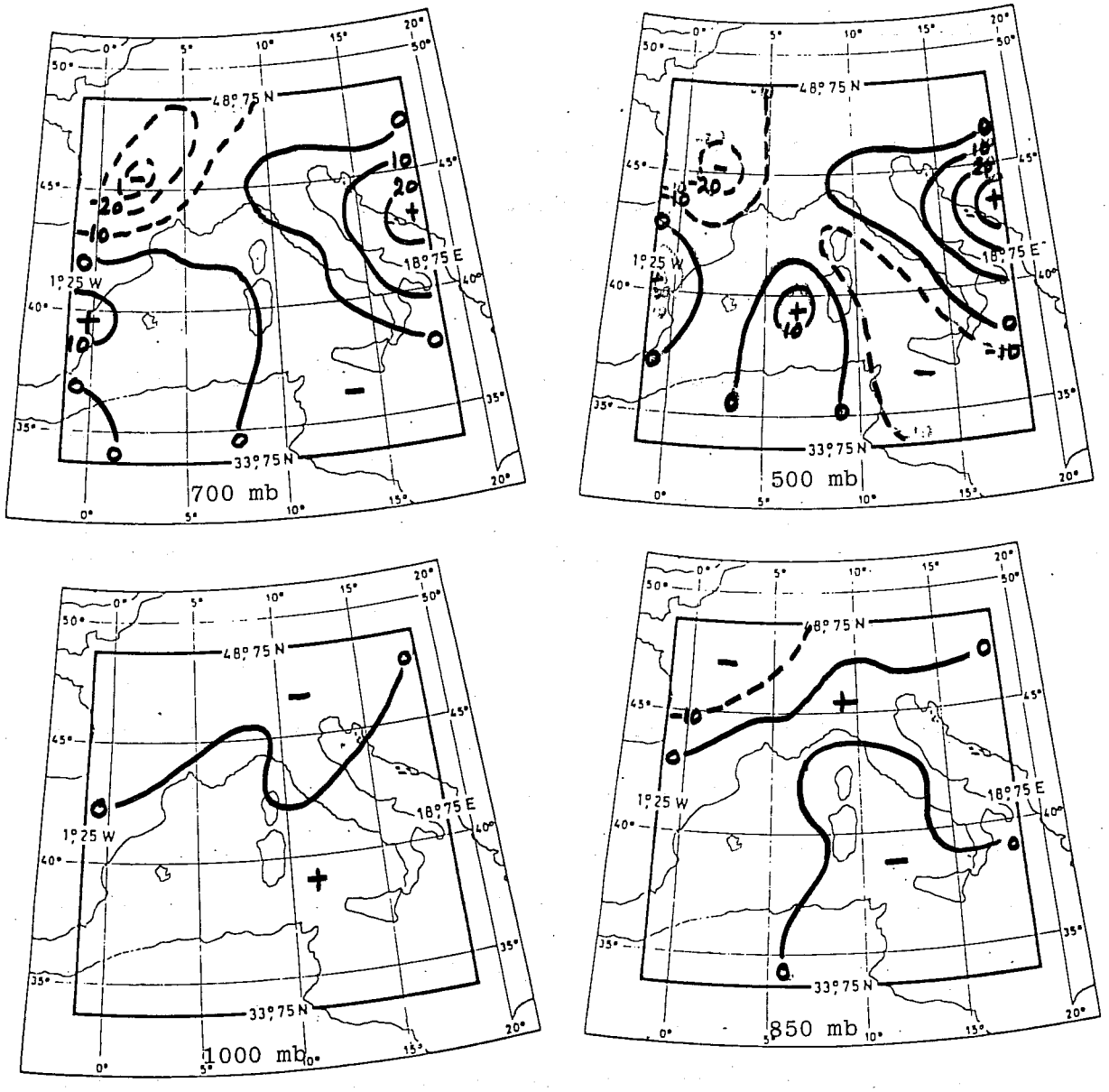

Fig. 10 Mean vertical velocity (10^{-4} mb/s) at the beginning of cyclogenesis in the lee of the Alps observed during the ALPEX SOP.

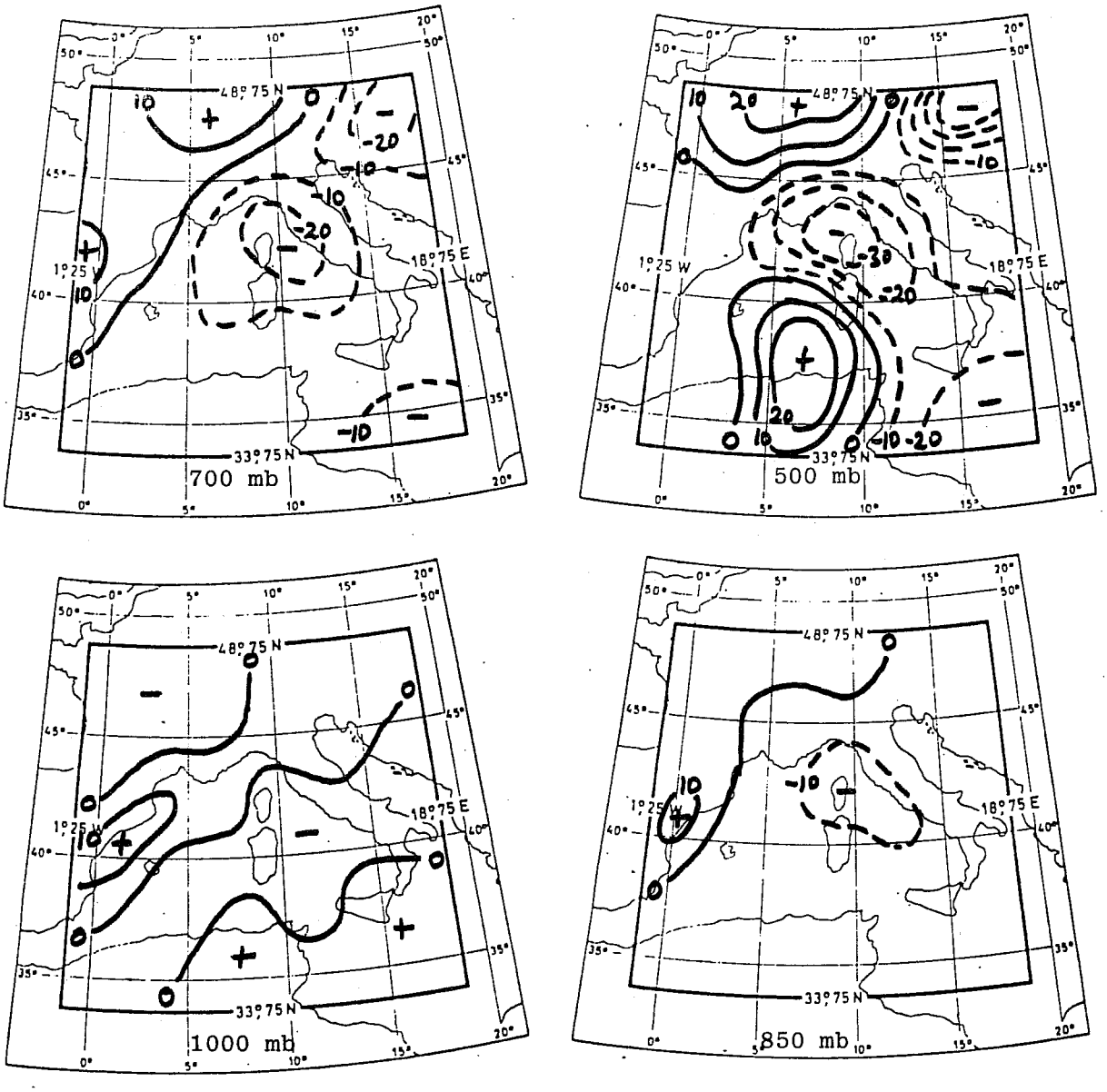

Fig. 11 Mean vertical velocity (10^{-4} mb/s) 12 hours after beginning of cyclogenesis in the lee of the Alps observed during the ALPEX SOP.

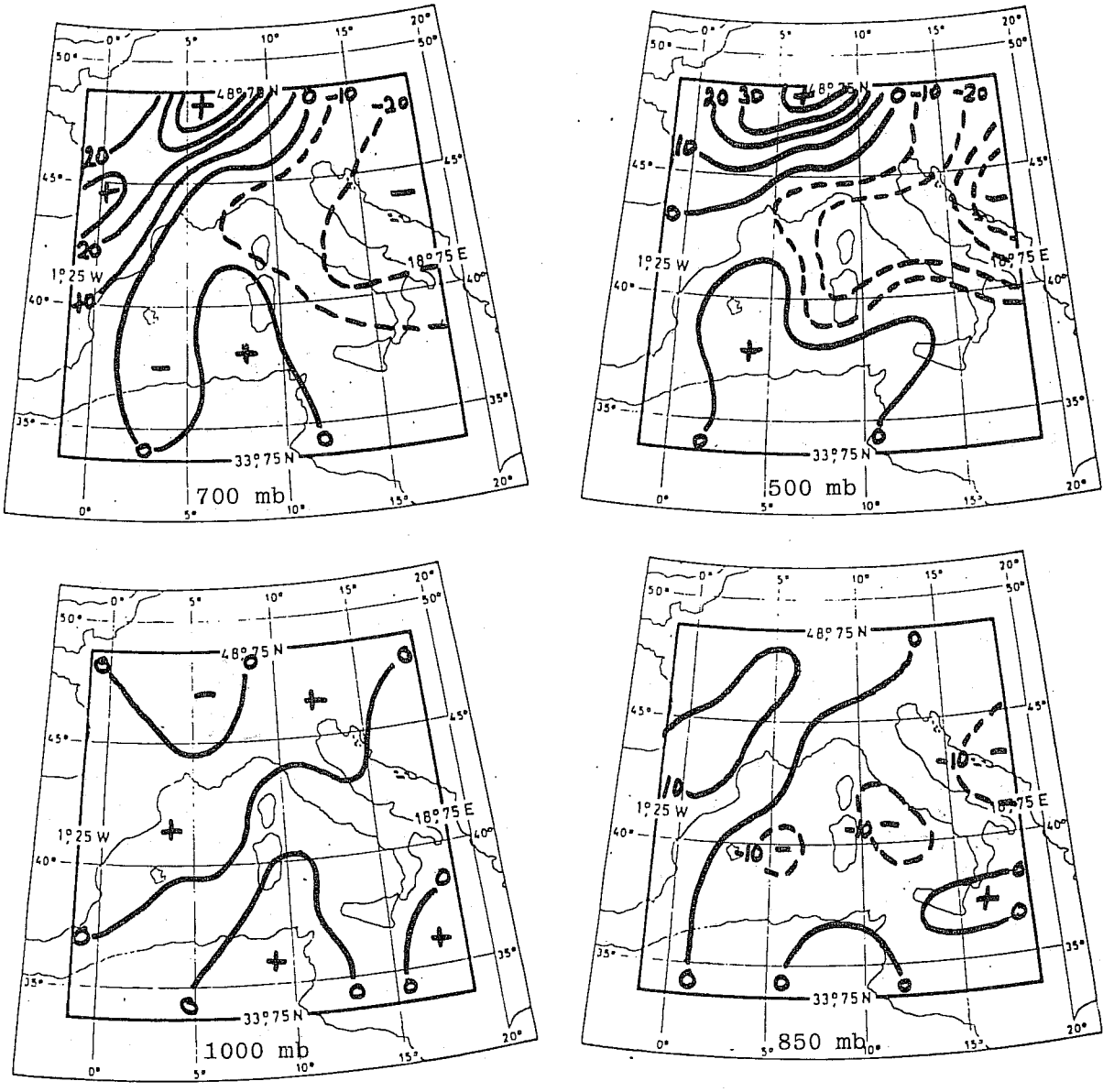

Fig. 12 Change of vertical velocity (10^{-4} mb/s) during the 12 hours after the beginning of cyclogenesis in the lee of the Alps observed ruing the ALPEX SOP.

4. THERMAL STRUCTURE

Synoptic evidence, as well as various investigations (Radinović, 1965; Tibaldi, 1980), shows that orographic cyclones have a rather specific thermal structure. In order to give an indication of the evolution of the thermal structure during cyclone development in the lee of the Alps, we will consider a few well known features.

Due to the surface conditions, the air mass over the western Mediterranean during the colder half of the year is considerably different from that over the surrounding land; the air over the sea is warmer, more humid and less stable. When cyclogenesis starts, the cyclonic circulation develops in a relatively homogeneous air mass. However, once rapid intensification takes place there is strong ascent and condensation, particularly over the southern slopes of the Alps, which causes the temperature, moisture and stability of the air in the western Mediterranean to change. As the cyclonic circulation enlarges, very warm dry air from north Africa is drawn into the forward side of the cyclone. At the same time there is cold air advection above the mountain level over the cyclone, while below that level the advection is obstructed. Later on, the cold air flows round the mountain range and penetrates into the western Mediterranean from the southwest (through the Rhone Valley) and the northeast (over the western part of Yugoslavia). Since these air masses have different tracks, their characteristics are slightly different by the time they meet in the lee of the Alps (Bergeron, 1928). Besides, many local effects of the mountains (such as wind channelling, cold air lakes, warm air islands, extensive cloud cover, heavy precipitation zones, intensified pressure gradient zones etc.) cause difficulties in making a frontal analysis. Since there is a lack of a reliable theory about the thermal structure of circulation systems in this region, it is the practice of

analysts to apply the simple Bergen frontal theory, and when the situation is very complicated they usually draw an occlusion in place of a complex front. As a result the analyses over southern Europe seems to be rather inconsistent and have a large number of occlusions.

On the basis of the analysis of the eight cases of cyclogenesis which occurred during the ALPEX SOP, we will now describe some additional features of the thermal structure of orographic cyclones. For this purpose the thickness changes in different layers for various sectors of the cyclones during their development have been calculated; the results are given in Tables 8 and 9.

Table 8 Average thickness changes during the first 12 hours of cyclogenesis (gpm)

Layer \ Points	0	W	S	E	N
850/1000	+2	-12	2	-3	-16
700/850	-9	-19	-3	0	-19
500/700	-38	-42	-11	6	-47
500/1000	-55	-61	-25	-6	-78

Table 9 Average thickness changes during 12 hours period of cyclogenesis (gpm)

Layer \ Points	0	W	S	E	N
850/1000	-8	-9	-7	-2	-4
700/850	-13	-15	-6	-9	-13
500/700	-36	-27	-24	-17	-21
500/1000	-59	-48	-35	-19	-39

From Table 8 it may be seen that during the first 12 hours of cyclogenesis there is slight warm advection at the centre of the cyclone only in the lowest layer. In the other layers there is cold advection and this intensifies upwards. The strongest advection of the cold air is in the northern and western sectors of the cyclone, i.e. on the windward side of the mountain range. Also notice that cold advection is present even in the southern sector, except in the lowest layer. In the eastern sector the situation is the opposite - slight advection of warm air aloft and cold advection in the lowest layers. This can be explained by the fact that often during cyclogenesis in the western Mediterranean a shallow cold air mass penetrates to the Balkan peninsular, while the south-westerly airflow remains aloft.

During the 12-24 hour period of cyclogenesis, cold advection takes place in all layers (Table 9). The greatest intensity is in the centre and the lowest in the eastern sector. It is also important to notice that there is a large difference in the intensity and volume of the cold and warm advection: compared to the cold advection, the warm advection is practically negligible. As a consequence, it is almost impossible to analyse a warm front caused by warm air 'pulled up' from the south. However a warm front is usually found as part of a wave formed on the cold front coming from the north or northwest after entering into the cyclone's circulation, but even then the warm front often has the characteristics of a cold front if the cyclone is fast moving.

5. KINETIC ENERGY CHANGE

For a detailed description of the mechanism of lee cyclogenesis, various terms in the equation for change of kinetic energy in a specified region have been computed using a similar approach to that followed by Palmen and Holopainen (1962) in their study of intensive cyclogenesis over the USA, and Radinović and Mesinger (1970) who investigated a rapid cyclone development over the western Mediterranean.

Computations were carried out for the region 33.75°-48.75°N, 1.25°W-18.75°E (shown in Figs. 1-12) which covers 2.78×10^{12} m^2. This area encompasses the western Mediterranean and the Alpine massif which, according to our findings so far, are the two major geographical factors affecting cyclone development in the western Mediterranean. Also the centre of cyclones developing in the lee of the Alps are approximately in the centre of this region. The area considered was fixed in time since the computations of kinetic energy change apply to when the cyclones are in their growing stage, and therefore mostly stationary.

The grid of points on which the computations are made consists of 6 x 8 points with a latitude-longitude spacing of 2.5°. The upper and lower boundaries of the computation box are the earth's surface (p_s) and the top of the troposphere (p_T) which for our purposes is taken to be 150 mb.

Using the usual notation, the total amount of kinetic energy (K) may be written as

$$K = \int_s \int_{p_T}^{p_s} \frac{1}{2} v^2 \frac{dp}{g} \, ds$$

By using pressure as the vertical coordinate, the equations of motion can be used to give an expression for the change of kinetic energy of the air in our box.

$$\frac{S}{g}\frac{\partial}{\partial t}\int_{p_T}^{p_s}\bar{K}dp = -\frac{L}{g}\int_{p_T}^{p_s}\widehat{Kv}_n dp + \frac{S}{g}[K\omega]_T$$

I II

$$-\frac{L}{g}\int_{p_T}^{p_s}(\hat{\phi}-\bar{\phi})\,\hat{v}_n dp - \frac{L}{g}\int_{p_T}^{p_s}\widehat{\phi''v_n''}dp$$

III IV

$$+\frac{S}{g}[\phi'\omega]_T - \frac{SR}{g}\int_{p_T}^{p_s}\frac{\overline{T'\omega'}}{p}dp$$

V VI

$$-\overline{S\,c\rho_s V_s^3}$$

VII

The notation used is that for any arbitary variable χ, $\bar{\chi}$ represents the mean value on an isobaric surface of area S and the deviation is given by $\chi'=\chi-\bar{\chi}$; similarly $\hat{\chi}$ represents the mean value around the boundary of length L and $\chi''=\chi-\hat{\chi}$ is the deviation of χ from the mean boundary value. Also c is the coefficient of friction for the earth's surface and V_s is the wind speed at anemometer level.

Each term in the above equation has been given a Roman numeral to facilitate identification. In this equation terms I and II represent the horizontal and vertical fluxes through the boundaries, terms III, IV, V and VI describe the transformation of the available potential energy to kinetic energy within the box, and term VII is the loss of kinetic energy due to friction at the earth's surface.

In Table 10 are shown the mean values of each of the terms in the equation. From this it can be seen that the total kinetic energy change at the beginning of cyclogenesis is higher than 12 hours later. Further it is apparent that nearly all this kinetic energy enhancement comes from the import of kinetic energy by the horizontal flux. In comparison the terms representing the net energy generation or transformation of available potential energy into kinetic energy are small and some even negative. This suggests that the main source of kinetic energy for lee cyclones is not the local baroclinicity, as might be expected, but rather the existing kinetic energy of the zonal flow. The role of the local baroclinicity seems to be to secure the necessary conditions for a specific redistribution of existing zonal flow kinetic energy.

Table 10. Mean values for the terms of the equation of kinetic energy change (10^{10} kj/S)

Term number	I	II	III	IV	V	VI	VII	Total
Onset of cyclogenesis	7.163	-0.023	0.267	-0.295	-0.618	-0.510	-0.056	3.078
12 hr after cyclogenesis started	7.678	0.118	0.616	-4.665	-0.991	-0.593	-0.325	1.920

6. MECHANISM OF DEVELOPMENT

One of the mechanisms for cyclogenesis in the western Mediterranean basin, which seems to be dominant, was described several decades ago by Radninović and Lalić (1959), and Radinović (1965). They suggested that lee cyclogenesis is associated with the existence of a trough in the 1000-500 mb thickness, situated to the west of the Alps, and its pronounced deformation as it approaches the mountain range. This deformation is indicated by a concentration of the thickness lines and intensification of the thermal wind which, according to the thermal development term in Sutcliffe's development theory, produces cyclonic vorticity at the surface. Several recent studies (Egger, 1972; Bleck, 1977; Buzzi and Tibaldi, 1978; McGinley, 1982) have supported this basic type of mechanism, though they have also shown that it is considerably more complex than first thought (see in particular McGinley, 1982).

A detailed investigation of the cases of cyclogenesis which occurred during the ALPEX SOP have shown that there are some additional effects involved in the mechanism of lee cyclogenesis which should be taken into consideration. In all eight cases the following features are, more or less, apparent:

(1) A diffluent upper level flow over the Alps and western Mediterranean immediately precedes lee cyclogenesis.

(2) During maximum development there is cold advection over the sea level cyclone.

(3) Two zones of concentrated thickness lines are evident during maximum development: one extending along the Alpine mountain range and the other along the north African coast.

The diffluent flow over the western Mediterranean was first described by Scherhag (1948) who observed that sea level cyclones frequently intensified where the upper level isobars diverged. With regard to this pattern, he expounded the proposition that 'divergent upper winds must produce in general a fall of pressure if they are not compensated by strong convergence below'.

Examples of the surface and 500 mb analyses during cyclogenesis are given in Figs. 13 and 14. First consider a long wave in the upper westerlies, with a cold slow moving trough situated immediately to the west of the Alps. If the terrain is flat, there would be a basic southwesterly flow with cyclonic curvature over the western Mediterranean basin. However, due to the mountain barrier, the meridional wind component and thickness gradient south of the mountains are decreased. Consequently the basic upper flow follows the Pyrenees and then curves anticyclonically around the Alps.

This idea can be described in terms of the gradient wind relationship.

$$KV^2 = - fV \quad g \left(\frac{\delta z}{\delta n}\right)_p$$

where K is the trajectory curvature (positive when cyclonic), V the wind speed and δn is the distance between contours separated by δz. This equation may be rewritten as

$$\delta n = \frac{g\delta z}{V(f+KV)}$$

and now illustrates that the distance between contours in a given area is prescribed by the wind speed and the trajectory curvature. If the wind speed exceeds the speed of movement of the wave pattern (i.e. the trajectory and streamline curvatures have the same sign) and the horizontal thickness gradient over the western Mediterranean is smaller than on the other side of the mountain barrier, then a diffluent upper level flow must appear in this region.

The existence of a diffluent flow over the western Mediterranean prior to cyclogenesis cannot be considered as a main cause of cyclogenesis. However there is some evidence that the diffluence contributes to cyclonic development by directing cold air round the mountain range (see Figs. 13 and 14).

When there is a cold air outbreak into the Alpine region from the northwest and north, the cold advection below the mean mountain level is directed mainly round the mountain range, while above this level the cold air is advected over the mountains into the the Mediterranean basin. This behaviour is illustrated in the series of charts shown in Figs. 15 to 18.

From these figures it may be seen that the cold advection aloft in the western Mediterranean basin takes place at the time of maximum cyclone development. The same behaviour has already been documented by Radinović, 1965 (Table 2) who showed that the cooling over Milan occurs in the higher layers earlier than in the lower ones and that the cooling persists from the beginning to the end of the pressure fall in the Gulf of Genoa.

It is usual to assume that the upper level advection of cold air into the western Mediterranean during cyclogenesis plays an important role in the lee cyclone development. We shall, therefore try to find an acceptable explanation using the same approach adopted by Radinović, 1965, i.e. by use of Sutcliffe's development theory.

The basic equation of Sutcliffe's theory is

$$\frac{\partial \eta_o}{\partial t} = -\underline{V} \cdot \nabla \eta - \frac{1}{f} \nabla^2 A_T + B \nabla^2 \overline{\omega(\gamma - \gamma_a)} - \frac{B}{C_p} \nabla^2 \frac{dQ}{dt} \qquad (1)$$

I II III IV V

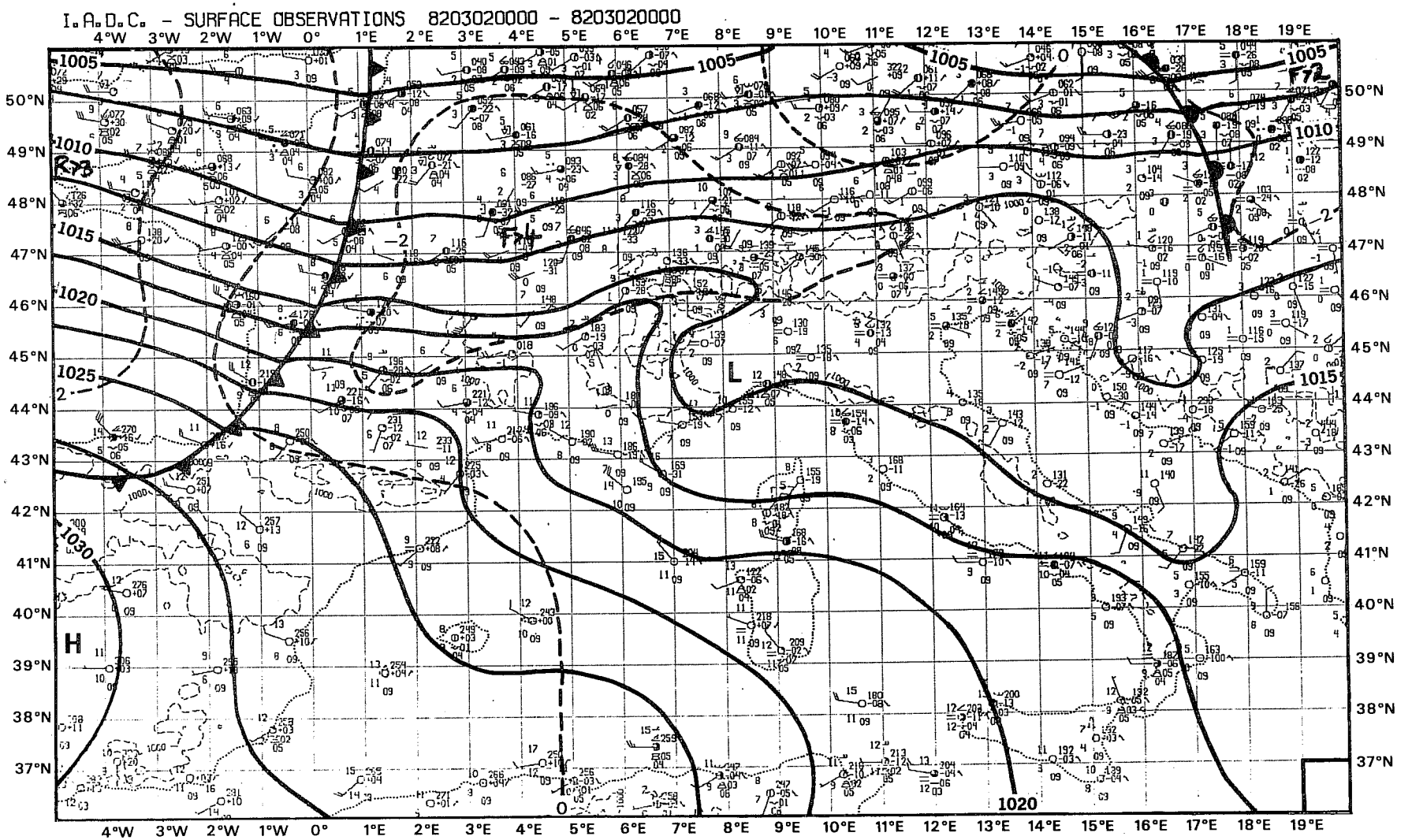

Fig. 13 Mean sea level pressure at 00Z 2 March 1982 with isopleths at 2.5 mb intervals.

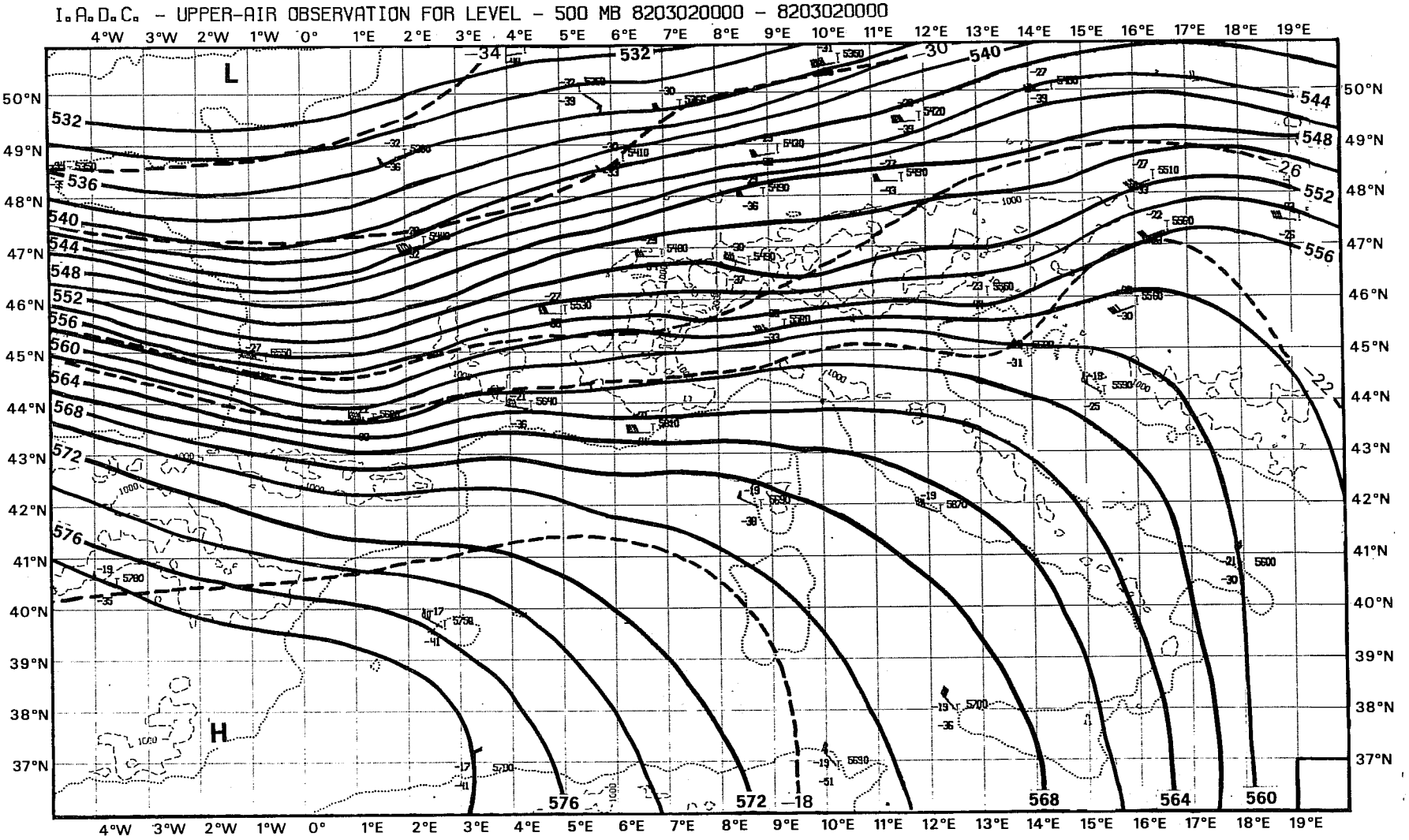

Fig. 14 500 mb contour and pressure at 00Z 2 March 1982 with isopleths at 3 dam and 2°C intervals.

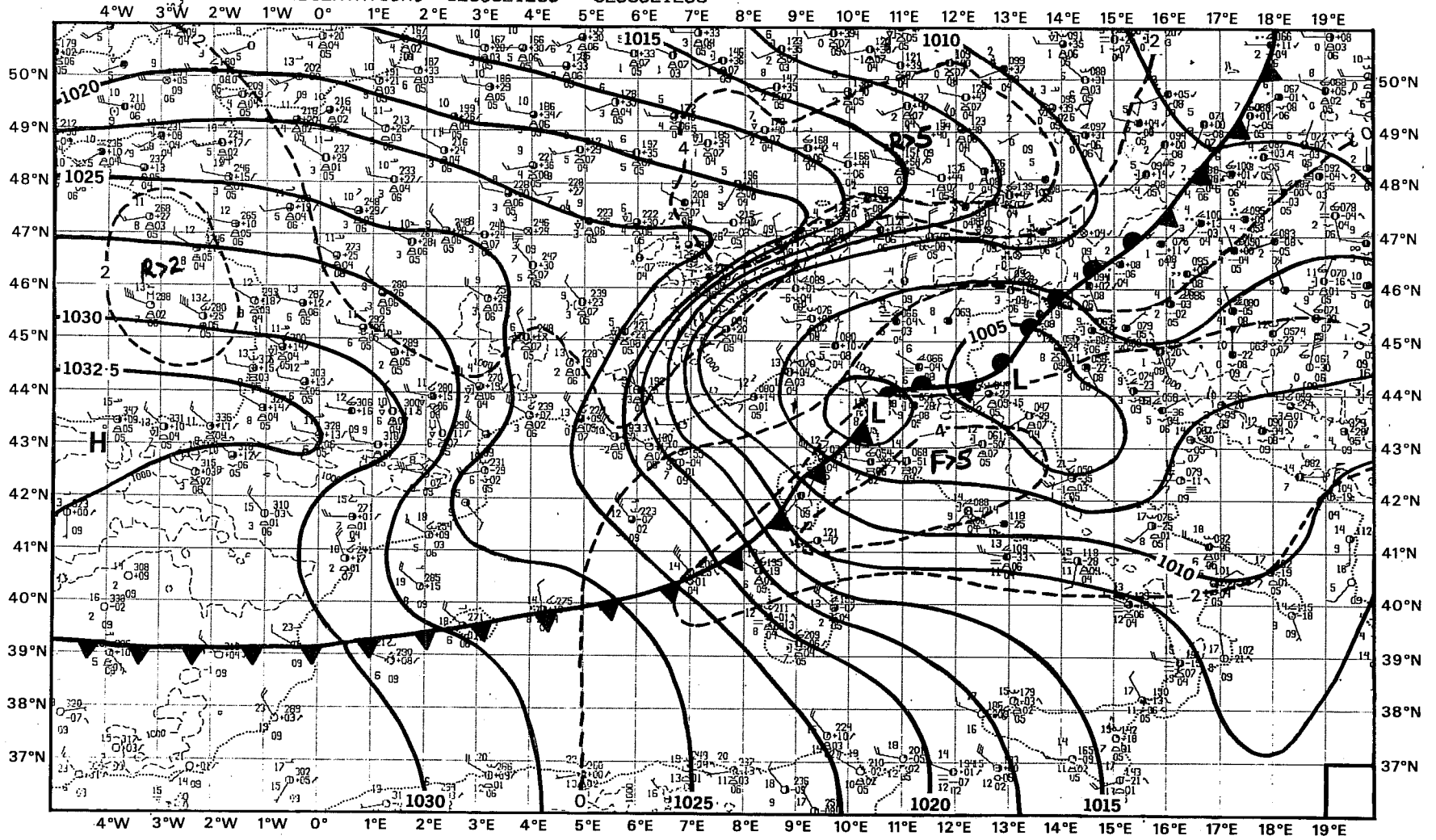

Fig. 15 Mean sea level pressure at 12Z 2 March with isopleths at 2.5 mb intervals.

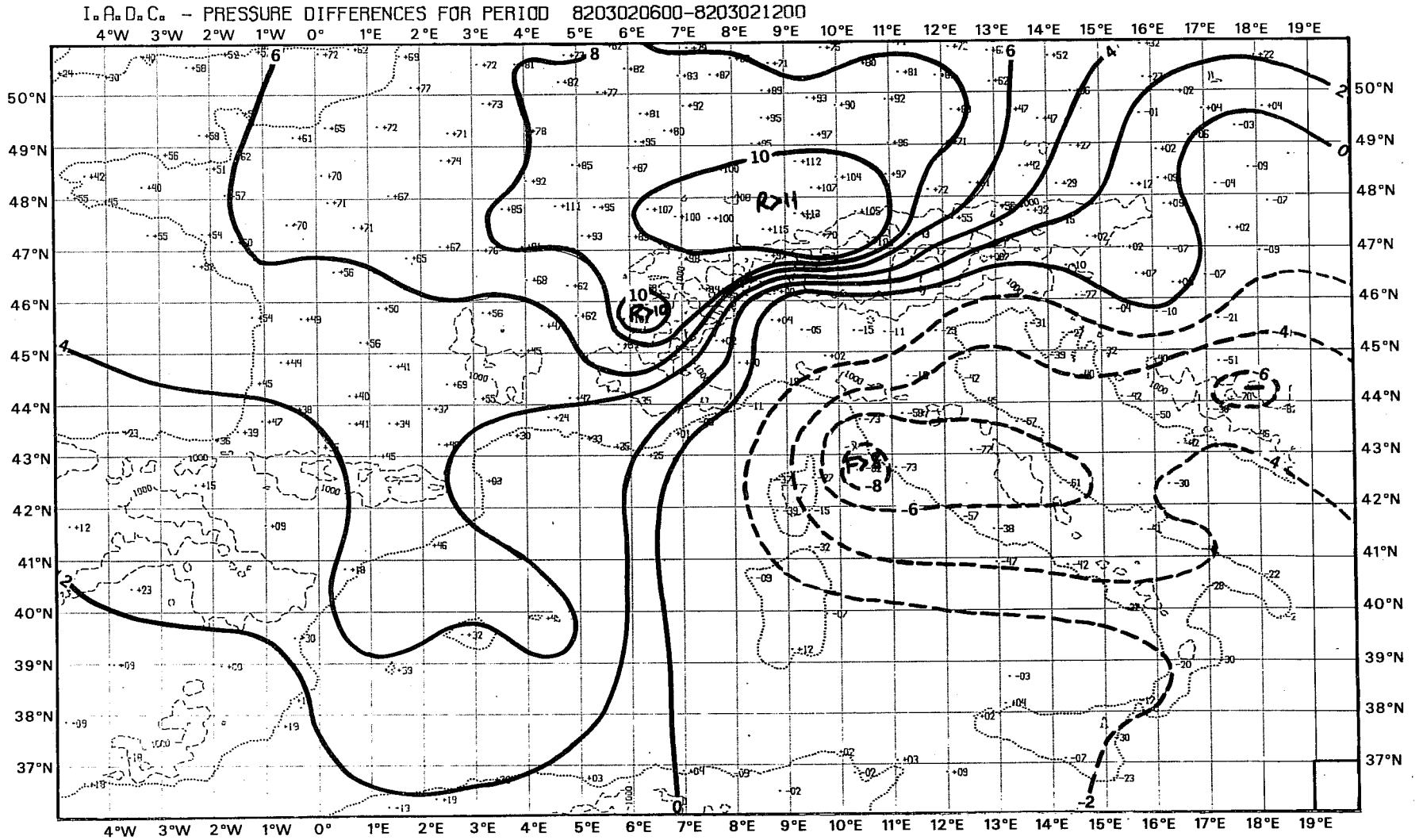

Fig. 16 Change in mean sea level pressure between 12Z and 06Z 2 March 1982 with isopleths at 2 mb intervals.

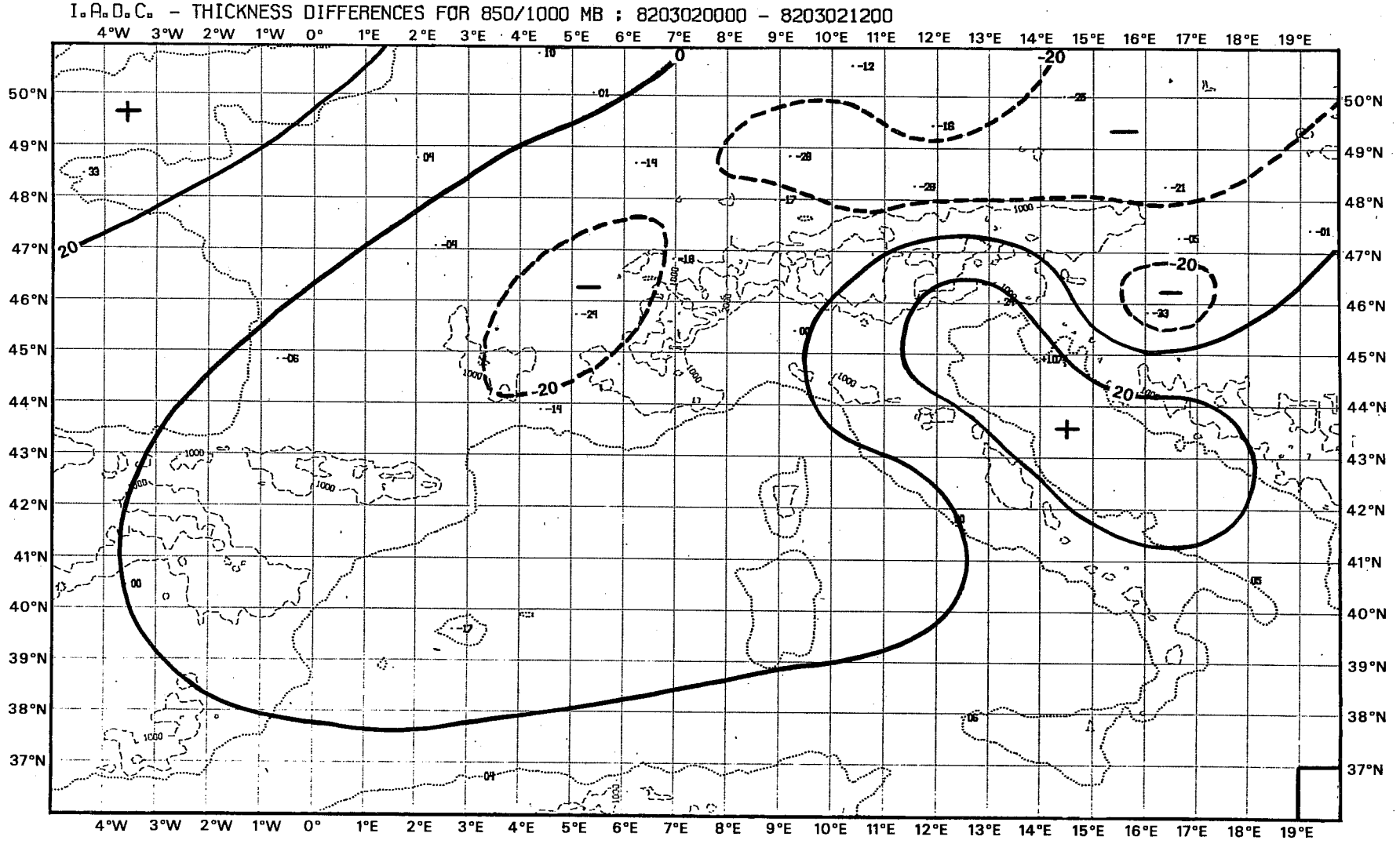

Fig. 17 Change in the 1000-850 mb thickness between 12Z and 00Z 2 March 1982 with isopleths at 20 m intervals.

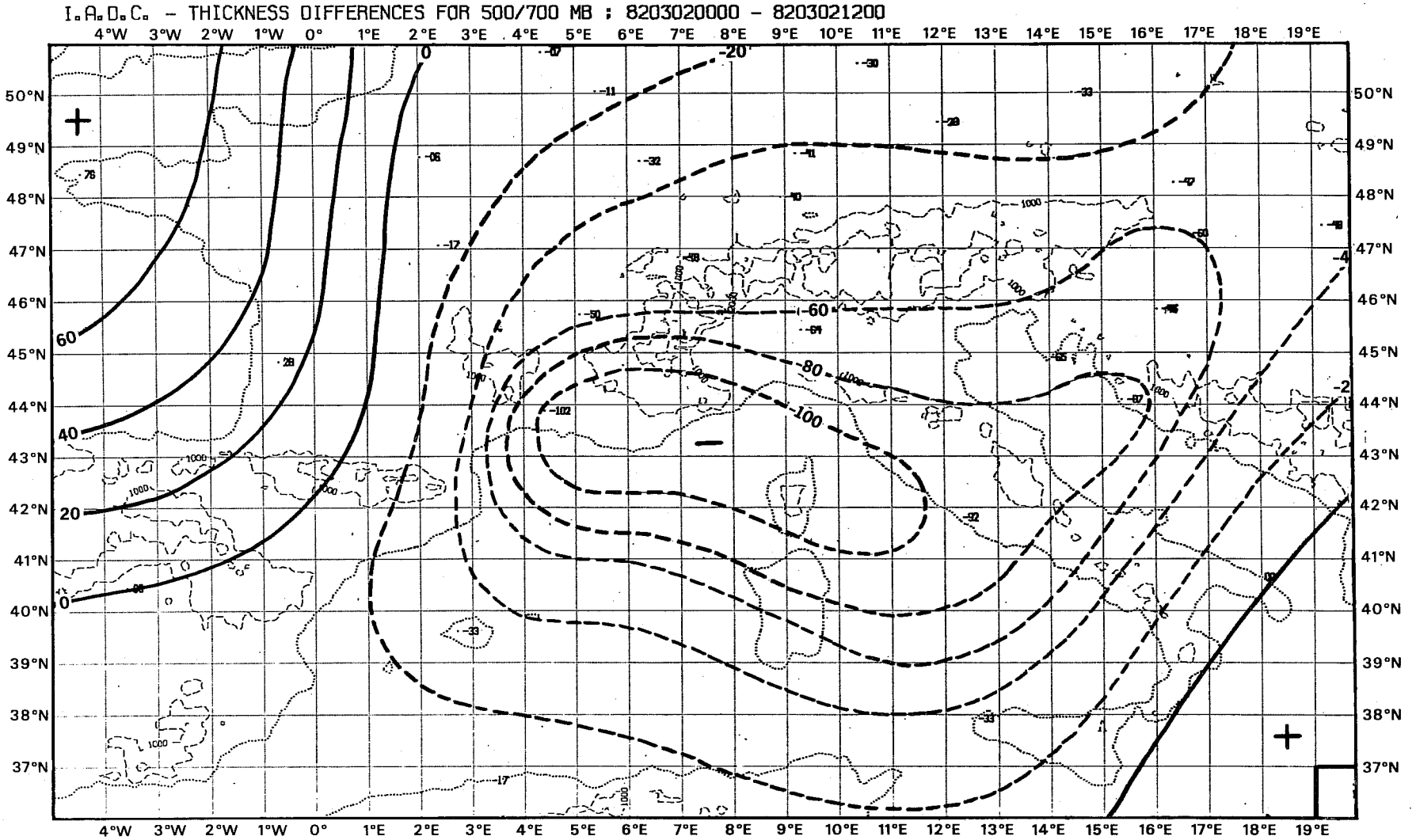

Fig. 18 Change in the 700-500 mb thickness between 12Z and 00Z 2 March 1982 with isopleths at 20 m intervals.

Here η_o and η are the absolute vorticity at sea level and the level of non-divergence, A_T is the thermal advection (thickness changes), ω is the 'omega' vertical velocity, γ and γ_a are the environmental and adiabatic lapse rates, $\frac{dQ}{dt}$ is the rate of heat supply and $B = \frac{R}{f} \ell n\ (p_o/p)$where p_o is the surface pressure. Each term in the equation is denoted by a Roman numeral to facilitate identification of the terms.

Earlier (Radinović, 1965) it was shown that the local vorticity changes due to non-adiabatic processes is less than the other contributions, so the last term in (1) can be neglected. At the same time both synoptic and statistical evidence support the view that the term III, the Laplacian of thermal advection, is considerably larger than terms II and IV; consequently these two terms have been neglected.

Investigations of the lee cyclones which occurred during the ALPEX SOP have shown that the cold air accumulation on the windward side, as well as its advection round the mountains in the lower layer of the troposphere, causes thickness lines to concentrate over the mountain range. Such a form of deformation makes term III a considerable size and contributes to cyclone development in the lee of the Alps. However, the existence of cold advection over the mountains directed towards the western Mediterranean shows that terms II and IV can give a significant contribution to cyclone development. It seems, therefore, that their omission from (1) cannot be unjustified.

All the terms in (1) can be evaluate with reasonable accuracy from synoptic data in regions where soundings are plentiful. Such a region is the Alpine outer region of the ALPEX SOP. Therefore terms I-IV have been computed by using data from the synoptic hour nearest the beginning of cyclogenesis and data from 12 hours later. This has been done for all eight cyclones. Some of the practical steps taken in the calculations are as follows:

(a) The vorticity is evaluate using a finite difference Laplacian with a gridlength of 500 km.

(b) Term III, representing the thermal advection in the layer 1000-500 mb, is evaluated by assuming that the thickness is changed by advection alone, that is

$$-\frac{1}{f}\nabla^2 A_T = \underline{V} \cdot \nabla\zeta_T - (\underline{V} \cdot \nabla\zeta_T + \frac{\delta\zeta_T}{\delta t}) \qquad (2)$$

$$III = III_1 \qquad III_2$$

where ζ_T is the thickness vorticity and δt is the time interval taken to be 12 hours in these calculations. In other words, it is supposed that the local vorticity change at the centre of the cyclone in the absence of orography is balanced by the thickness advection term. In that case the total value of the terms within the parenthesis on the righthand side of (1) is equal to zero. On the other hand, in areas where high mountains exist the advection will be stopped in the lower layers and only take place higher up. A real thermal advection, therefore, corresponds to the difference between the local change of thickness vorticity and its advection, as shown in (2).

(c) The vertical velocity in term IV is computed from the absolute vorticity equation

$$\frac{1}{\eta}\frac{d\eta}{dt} \approx \frac{1}{\eta}\frac{\partial\eta}{\partial t} = \frac{\partial\omega}{\partial p} \qquad (3)$$

applied at the 700 mb level. Assuming that during the first 12 hours of cyclogenesis the vorticity change at 500 mb, compared to that at the surface, is small and that the vertical velocity at the surface is zero, then (3) may be rewritten as

$$\bar{\omega} \approx \frac{\delta p}{\eta_o}\frac{\delta\eta_o}{\delta t}$$

where $\bar{\omega}$ is the mean vertical velocity in the 1000-500 mb layer.

(d) The mean environmental lapse rate δ in term IV is computed from the difference in thickness in the layers 1000-700 mb and 700-500 mb (Radinović, 1966); denoting these thicknesses by $Z_{10/7}$ and $Z_{7/5}$ we then have

$$\gamma = -\frac{\partial T}{\partial p}$$

$$= \frac{g}{2.5 \times 10^3 R}\left[Z_{10/7}\left(\ell n \frac{700}{1000}\right)^{-1} - Z_{7/5}\left(\ell n \frac{500}{700}\right)^{-1}\right] \text{ K kg}^{-1} \text{ m s}^2$$

Using these assumptions, all the terms in (1) for the eight cases of cyclogenesis have been calculated, and these are displayed in Table 11. From this it may be seen that the intensity of cyclogenesis, represented by the values in column I, is approximately equal to the sum of the terms which describe the cyclogenetic effects (columns II to IV).

Table 11. The values of individual terms of equation (1) representing the contributions to cyclogenesis in the West Mediterranean ($10^{-9}s^{-2}$)

Case No.	Date	Period	Cyclogenetic effects				
			I	II	III_1	III_2	IV
1	2.3.82	00-12 GMT	2.0	3.0	-2.0	1.0	0.3
2	4.3.82	00-12 GMT	2.7	1.6	-1.3	1.7	0.7
3	11.3.82	00-12 GMT	3.3	2.0	-0.9	1.1	0.6
4	13.3 82	00-12 GMT	2.6	1.8	-2.2	1.5	0.2
5	17.3 82	12-24 GMT	1.8	1.7	-0.6	1.5	0.3
6	20.3 82	00-12 GMT	0.6	0.4	-0.9	1.3	0.1
7	24.4 82	00-12 GMT	3.0	1.4	-1.3	2.2	0.4
8	30.4 82	00-12 GMT	1.1	0.5	-1.1	0.4	0.2
Mean values			2.14	1.55	-1.29	1.34	0.35

The values in column II represent the vorticity advection at 500 mb and it shows that this provides the highest contribution to the cyclogenesis. In column III, are the values corresponding to thickness advection, and in all cases they are negative showing that thickness advection produces anticyclonic development. However, this effect is completely neutralised by the thickness field deformation in the lower layers caused by the orography, as seen in column III_2. The last column represents the cyclogenetic effect caused by the vertical notion of air in an unstable atmosphere. This effect is 4-5 times smaller than the advective ones, but it is still significant and should not be ignored.

The results of this study indicate that there may be compensating factors at different levels: generation of vorticity by thermal advection at low levels and advection of vorticity by the large scale flow at upper levels. This confirms the findings of Buzzi and Tibaldi (1978).

Finally the cold advection above mountain top level and its blocking below that level during the first stage of cyclogenesis, as described earlier, leads to the formation of two thermal jets in the 1000-500 mb thickness. This process is clearly illustrated in Figs. 19 and 20.

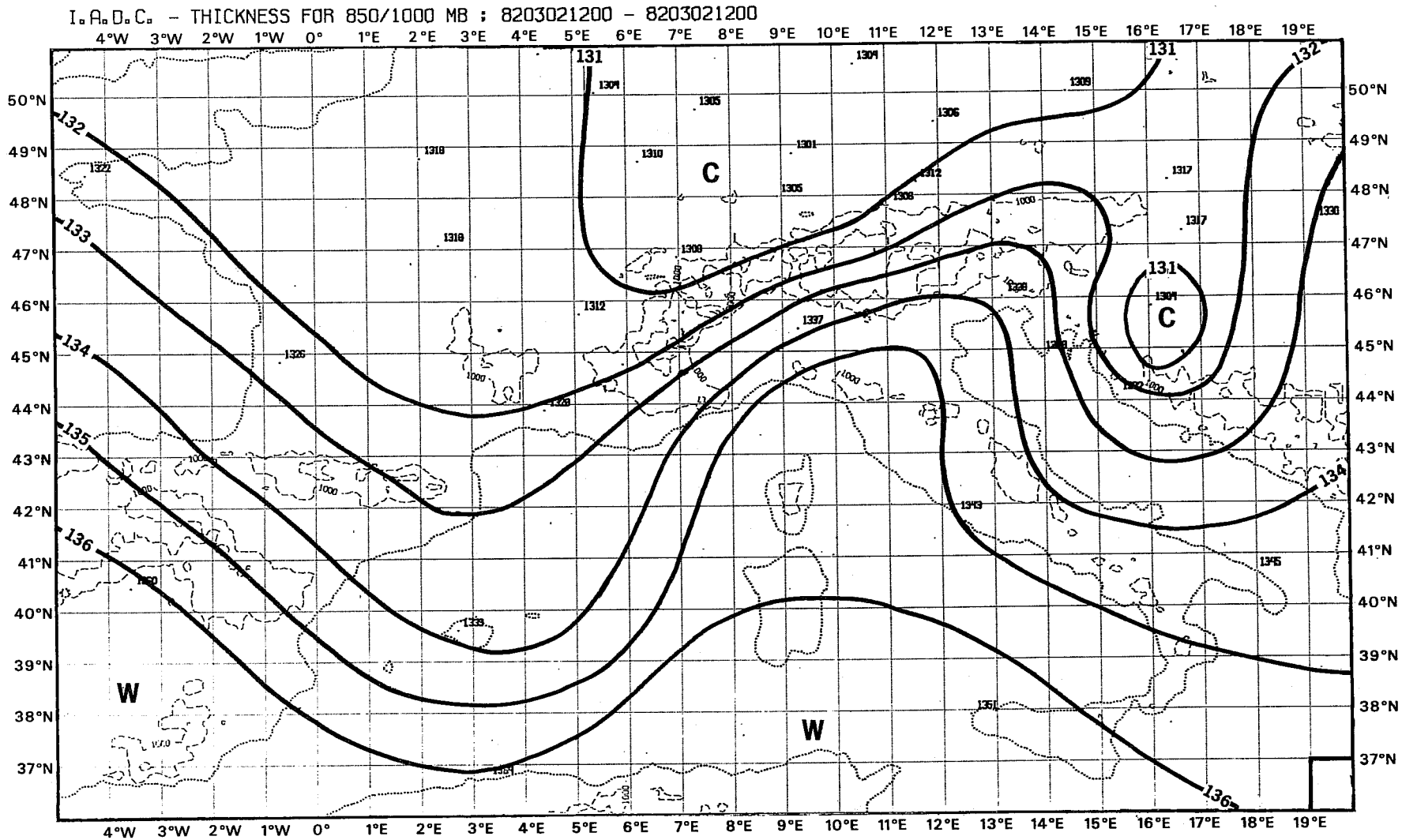

Fig. 19 1000-850 mb thickness at 12Z 2 March 1982 with isopleths at 1 dam intervals.

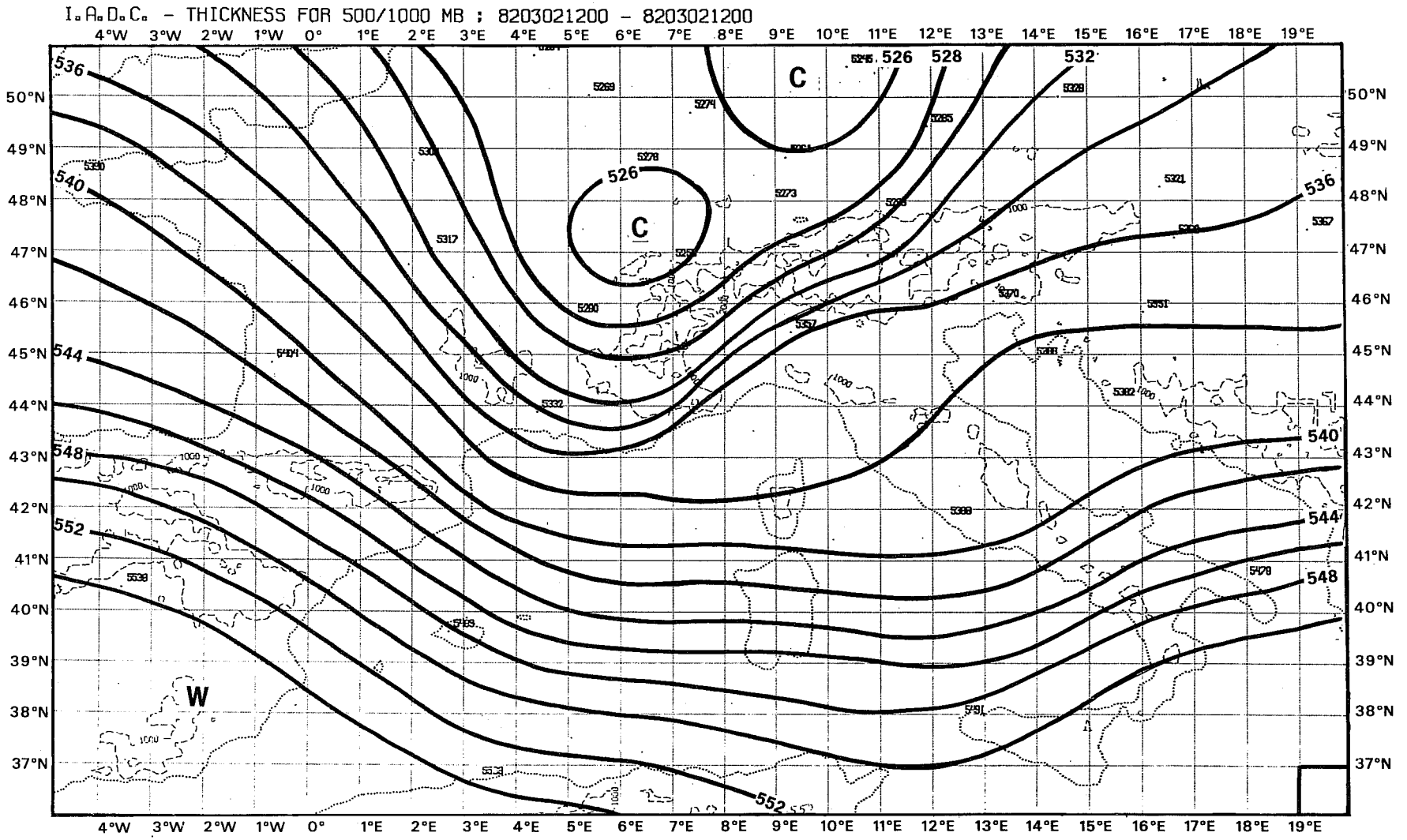

Fig. 20 1000-500 mb thickness at 12Z 2 March 1982 with isopleths at 2 dam intervals.

7. COMPARISON WITH OTHER TYPES OF EXTRATROPICAL CYCLONES

The difference in the mechanism for the three types of cyclogenesis is revealed by a comparison of their dynamic and synoptic characteristics which appear on synoptic charts. On the basis of the work of Petterssen and Smebye (1971), the present study and a number of other studies concerned with lee cyclogenesis, the pertinent characteristics of the three types of extratropical cylone development will be summarised. In this comparison th different types of cyclogenetic mechanisms are called Types A, B and C.

Type A - amplifying frontal wave

Type B - disturbance in the upper troposphere

Type C - orographic disturbance

(1) Initial synoptic conditions

A - baroclinic instability of frontal wave;

B - disturbance in the upper troposphere accompanied by an augmentation of the baroclinicity (medium and upper troposphere);

C - orographic blocking of cold airmass accompanied by an augmentation of the baroclinicity in the lower troposphere (Radinović, 1965; Buzzi and Tibaldi, 1978; McGinley, 1982).

(2) Energy source

A - kinetic energy produced through a reduction of the baroclinicity locally within the domain of the frontal wave;

B - kinetic energy imported into the cyclone domain, mainly from the jet-stream region;

C - kinetic energy produced through a reduction of the baroclinicity locally within the domain of the orographic obstacle and redistribution of kinetic energy of the zonal flow (see Sect.5 in this report; Tibaldi; Buzzi and Malguzzi 1980; McGinley, 1982).

(3) Commencement of development

A - development commences under a more or less straight upper current (without appreciable vorticity advection) in the zone of maximum baroclinicity (frontal region);

B - development commences when a pre-existing upper trough, with strong vorticity advection on its forward side, spreads over a low level area of warm advection (or near absence of cold advection) in which fronts may or may not be present;

C - development commences when a pre-existing upper trough approaching the mountain ranges starts undergoing a deformation caused by cold air mass blocking and its deflection round the obstacle. The deformation is accompanied by an augmentation of the baroclinicity within the domain of the obstacle and the creation of the negative thickness vorticity in the layer below the mountain top level in the lee of the mountain (Radinović, 1965; Egger, 1972; Tibaldi, 1980).

(4) Upper trough and low-system connection

A - no upper cold trough is present initially, but one develops as the low-level cyclone intensifies; the separation between the upper trough and the low level cyclone remains almost unchanged until peak intensity is reached;

B - the separation between the upper trough and the low level system decreases rapidly while the cyclone intensifies, and the axis tends to a vertical position as the cyclone approaches peak intensity;

C - the separation between the upper trough, with its axis on the windward side, and the low-level cyclone in the lee of the obstacle remains essentially unchanged until the cold air mass starts flowing over the obstacle and then it decreases rapidly (Radinović, 1965; Buzzi and Rizzi, 1975).

(5) Vorticity advection

A - the amount of vorticity advection aloft is very small initially, and remains relatively small throughout the development;

B - the amount of vorticity advection aloft is very large initially and decreases toward the time when peak intensity is reached;

C - the amount of vorticity advection aloft is small initially and remains small until the cold air starts flowing over the obstacle; then a pre-existing upper trough moves into the domain of the low level cyclone and positive vorticity advection aloft increases rapidly. (see Sect.6 of this paper and McGinley, 1982).

(6) Thermal advection

A - the thermal advection due to baroclinic instability is very pronounced and the main contribution to the intensification of the cyclone comes from the thermal advection;

B - the amount of thermal advection is small initially and increases as the low level cyclone intensifies;

C - the amount of thermal advection is negligible initially since the low level cyclone starts developing in a thermally uniform air mass; but there are two critical times when the thermal advection changes radically: first, when the cold air starts penetrating in the rear of the low-level cyclone and second when cold air starts flowing over the obstacle. (Radinović, 1962; Buzzi and Tibaldi, 1978; McGinley, 1982).

(7) Baroclinicity

A - the amount of baroclinicity in the lower troposphere is large initially and decreases as the wave occludes;

B - the amount of baroclinicity in the lower troposphere is relatively small initially and increases as the storm intensifies;

C - the amount of baroclinicity in the lower troposphere is large initially and increases until peak intensity is reached and then decreases. (Radinović, 1965; Tibaldi; Buzzi and Malguzzi, 1980; McGinley, 1982).

(8) Front evolution

A - cold and warm fronts as well as a warm sector are usually well defined throughout the development and the end result of the development is an occlusion of the classical type;

B - no one front or several fronts at the same time can be identified in the domain of the cyclone; the end result of the development is a thermal structure that resembles the classical occlusion;

C - no fronts initially, then warm advection on the forward side of the cyclone increases as the low level cyclone intensifies but it is difficult to identify a warm front; after cold air penetration a cold front passes from the rear of the cyclone to its forward side; the end of the development is usually an occlusion of the orographic type (Bergeron, 1928).

(9) Movement

A - moves relatively fast initially in the direction of the upper flow and as the disturbance develops aloft it slows down;

B - moves relatively fast initially with the speed gradually decreasing as the cyclone approaches peak intensity when it becomes almost stationary;

C - stays stationary until the steering effect (in terms of Sutcliffe's theory of development) exceeds the orographic effect. (Radinović and Lalić 1959; Speranza, 1975; McGinley, 1982).

(10) Cut-off

A - rarely cut-off in the upper troposphere and when it happens it occurs in a stage of occlusion;

B - it cuts-off regularly as the cyclone approaches peak intensity; it is caused by intense cold advection in the rear and continuing warm advection in the upper troposphere on the forward side of the cyclone;

C - cut-off regularly produced at the time of peak intensity and it is caused chiefly by intense a cold advection by the sea level pressure ridge on the windward side of mountain obstacle which builds up as a consequence of cold air accumulation. (See Sect.2 in this report).

8. CONCLUSIONS

From the results described in this paper, we can conclude that the evidence drawn from the cases of lee cyclogenesis which occurred during the ALPEX SOP supports Danielsen's ideas (1973) that "the baroclinic instability determines when and the mountains determine where the cyclone will form." That is an upper air trough is associated with a cold air mass in the lower troposphere and strong cyclonic vorticity in the middle of the troposphere. As the trough progresses the effect of upper air cyclonic vorticity is usually compensated by cold advection in the lower layers. However when it passes over the mountain range the upper air cyclonic vorticity is not adequately compensated and baroclinic instability is triggered. As a consequence low level cyclogenesis occurs in the lee of the obstacle.

Another conclusion from this study is that the mechanism of lee cyclogenesis is rather specific. It seems justified, therefore, to treat the orographic cyclone as a separate type of extratropical cyclone.

Acknowledgement

The author thanks Dr. L. Bengtsson, Director of ECMWF for his kind invitation to the Centre which made these studies possible and to Dr. D.M. Burridge, Head of Research, for providing the facilities. I am thankful to Dr. R.W.Riddaway who helped edit this paper.

References

Bergeron, T., 1928: Über die dreidimensionale verknupfende Wetteranalyse. I. Geofys.Publ., Oslo 5, No.6, 1-111.

Bleck, R., 1977: Numerical simulation of lee cyclogenesis in the Gulf of Genoa. Mon.Wea.Rev., 105, 428-445.

Buzzi, A. and S. Tibaldi, 1978: Cyclogenesis in the lee of the Alps: A case study. Quart.J.Roy.Meteor.Soc., 104, 271-287.

Buzzi, A. and E. Tosi, 1982: Lee cyclogenesis during the ALPEX SOP. ALPEX Preliminary Results, J.P. Kuettner, ed. GARP-ALPEX No.7, WMO, Geneva, 41-48.

Danielsen, E., 1973: Cyclogenesis in the Gulf of Genoa. Mesoscale Meteorological Phenomena, Proc. 1973 CNR Summer School, 189-192.

Dell'Osso, L. and S. Tibaldi, 1982: Some preliminary modelling results on an ALPEX case of lee cyclogenesis. ALPEX Preliminary Results, J.P. Kuettner, ed. GARP-ALPEX No.7, WMO, Geneva, 3-19.

Egger, J., 1972: Incorporation of steep mountains in numerical forecasting models. Tellus, 24, 324-335.

Kasahara, A., 1980: Influence of orography on the atmospheric general circulation. GARP Publications Series No. 23, 1-49.

Illari, L., P. Malguzzi and A. Speranza, 1981: On breakdowns of the Westerlies. Geophys.Astrophys.Fluid Dyn, 17, 27-49.

Jansa, A. and C. Ramis, 1982: Catalonian-Balearic Sea cyclogenesis. ALPEX Preliminary Results, J.P. Kuettner, ed. GARP-ALPEX No.7, WMO, Geneva, 49-61.

Lüdecke, C., 1982: Description of a cyclone in lee of the Alps on April 25, 1982. ALPEX Preliminary Results, J.P. Kuettner, ed. GARP-ALPEX No.7, WMO, Geneva, 77-86.

Mattocks, C., 1982: A percursory case study of lee cyclogenesis. ALPEX Preliminary Results, J.P. Kuettner, ed. GARP-ALPEX No.7, WMO, Geneva, 62-76.

McGinley, J., 1982: A diagnosis of Alpine lee cyclogenesis. Mon.Wea.Rev., 110, 1271-1287.

Palmén, E. and E.O. Holopainen, 1962: Divergence, vertical velocity and conversion between potential and kinetic energy in an extratropical disturbance. Geophysica 8 (2), 89-113.

Petterssen, S. and S.J. Smebye, 1971: On the development of extratropical cyclones. Quart.J.R.Met.Soc., 97, 457-482.

Pham, H.L., 1982: Numerical simulation of a case of cyclogenesis during ALPEX. ALPEX Preliminary Results, J.P. Kuettner, ed. GARP-ALPEX No.7, WMO, Geneva, 36-40.

Radinović D., 1962: Analysis of the cyclogenetic effects in the West Mediterranean. VI Internat. Meeting of Alpine Meteorology.

Radinović D., 1965: On forecasting of cyclogenesis in the West Mediterranean and other areas bounded by mountain ranges by baroclinic model. Arch.Meteor.Geophys.Boklim.,Ser. A, 14, 279-299.

Radinović D., 1965a: Cyclonic activity in the western Mediterranean. Fed.Hydromet. Institute, Belgrade, Memoires No.7, 57pp.

Radinović D., 1966: Orographic influence on the air stream deformation in variable static stability of the atmosphere. Die 3 Konferenz für Karpatenmeteorologie, SHMZ, Beograd, 265-271.

Radinović D. and D. Lalic, 1959: Cyclonic activity in the western Mediterranean. Fed.Hydromet.Institute, Belgrade, Memoirs No.7, 57p.

Radinović D. and F. Mesinger, 1970: Divergence, vertical velocity ad energy conversion in the West Mediterranean during cyclone development of 24 October 1964. Faculty of Sciences, Belgrade, Papers No.7, 117pp.

Scherhag, R., 1948: Neue Methoden der Wetteranalyse und Wetterprognose. Springer, Berlin, 424pp.

Speranza, A., 1975: The formation of baric depressions near the Alps. Annali di Geofisica, 28, 177-217.

Tibaldi, S., 1980: Cyclogenesis in the lee of orography and its numerical modelling, with special reference to the Alps. GARP Publ.Series No.23, WMO, Geneva, 207-232.

Tibaldi, S., A. Buzzi and P. Malguzzi, 1980: Orographically induced cyclogenesis: analysis of numerical experiments. Mon.Wea.Rev., 108, 1302-1314.

ECMWF PUBLISHED TECHNICAL REPORTS

No.1 A Case Study of a Ten Day Prediction

No.2 The Effect of Arithmetic Precisions on some Meteorological Integrations

No.3 Mixed-Radix Fast Fourier Transforms without Reordering

No.4 A Model for Medium-Range Weather Forecasting - Adiabatic Formulation

No.5 A Study of some Parameterizations of Sub-Grid Processes in a Baroclinic Wave in a Two-Dimensional Model

No.6 The ECMWF Analysis and Data Assimilation Scheme - Analysis of Mass and Wind Fields

No.7 A Ten Day High Resolution Non-Adiabatic Spectral Integration: A Comparative Study

No.8 On the Asymptotic Behaviour of Simple Stochastic-Dynamic Systems

No.9 On Balance Requirements as Initial Conditions

No.10 ECMWF Model - Parameterization of Sub-Grid Processes

No.11 Normal Mode Initialization for a Multi-Level Gridpoint Model

No.12 Data Assimilation Experiments

No.13 Comparisons of Medium Range Forecasts made with two Parameterization Schemes

No.14 On Initial Conditions for Non-Hydrostatic Models

No.15 Adiabatic Formulation and Organization of ECMWF's Spectral Model

No.16 Model Studies of a Developing Boundary Layer over the Ocean

No.17 The Response of a Global Barotropic Model to Forcing by Large-Scale Orography

No.18 Confidence Limits for Verification and Energetic Studies

No.19 A Low Order Barotropic Model on the Sphere with the Orographic and Newtonian Forcing

No.20 A Review of the Normal Mode Initialization Method

No.21 The Adjoint Equation Technique Applied to Meteorological Problems

No.22 The Use of Empirical Methods for Mesoscale Pressure Forecasts

No.23 Comparison of Medium Range Forecasts made with Models using Spectral or Finite Difference Techniques in the Horizontal

No.24 On the Average Errors of an Ensemble of Forecasts

ECMWF PUBLISHED TECHNICAL REPORTS

No.25 On the Atmospheric Factors Affecting the Levantine Sea

No.26 Tropical Influences on Stationary Wave Motion in Middle and High Latitudes

No.27 The Energy Budgets in North America, North Atlantic and Europe Based on ECMWF Analyses and Forecasts

No.28 An Energy and Angular-Momentum Conserving Vertical Finite-Difference Scheme, Hybrid Coordinates, and Medium-Range Weather Prediction

No.29 Orographic Influences on Mediterranean Lee Cyclogenesis and European Blocking in a Global Numerical Model

No.30 Review and Re-assessment of ECNET - a Private Network with Open Architecture

No.31 An Investigation of the Impact at Middle and High Latitudes of Tropical Forecast Errors

No.32 Short and Medium Range Forecast Differences between a Spectral and Grid Point Model. An Extensive Quasi-Operational Comparison

No.33 Numerical Simulations of a Case of Blocking: the Effects of Orography and Land-Sea Contrast

No.34 The Impact of Cloud Track Wind Data on Global Analyses and Medium Range Forecasts

No.35 Energy Budget Calculations at ECMWF: Part I: Analyses

No.36 Operational Verification of ECMWF Forecast Fields and Results for 1980-1981

No.37 High Resolution Experiments with the ECMWF Model: a Case Study

No.38 The Response of the ECMWF Global Model to the El-Nino Anomaly in Extended Range Prediction Experiments

No.39 On the Parameterization of Vertical Diffusion in Large-Scale Atmospheric Models

No.40 Spectral characteristics of the ECMWF Objective Analysis System

No.41 Systematic Errors in the Baroclinic Waves of the ECMWF Model

No.42 On Long Stationary and Transient Atmospheric Waves

No.43 A New Convective Adjustment Scheme

No.44 Numerical Experiments on the Simulation of the 1979 Asian Summer Monsoon

No.45 The Effect of Mechanical Forcing on the Formation of a Mesoscale Vortex

ECMWF PUBLISHED TECHNICAL REPORTS

No.46 Cloud Prediction in the ECMWF Model

No.47 Impact of Aircraft Wind Data on ECMWF Analyses and Forecasts during the FGGE Period, 8-19 November 1979 (not on WP, text provided by Baede)

No.48 A Numerical Case Study of East Asian Coastal Cyclogenesis

No.49 A Study of the Predictability of the ECMWF Operational Forecast Model in the Tropics

No.50 On the Development of Orographic Cyclones